RANDOM WALK MODELS OF NETWORK FORMATION AND SEQUENTIAL MONTE CARLO METHODS FOR GRAPHS

BENJAMIN BLOEM-REDDY AND PETER ORBANZ

University of Oxford and Columbia University

We introduce a class of generative network models that insert edges by connecting the starting and terminal vertices of a random walk on the network graph. Within the taxonomy of statistical network models, this class is distinguished by permitting the location of a new edge to explicitly depend on the structure of the graph, but being nonetheless statistically and computationally tractable. In the limit of infinite walk length, the model converges to an extension of the preferential attachment model—in this sense, it can be motivated alternatively by asking what preferential attachment is an approximation to. Theoretical properties, including the limiting degree sequence, are studied analytically. If the entire history of the graph is observed, parameters can be estimated by maximum likelihood. If only the final graph is available, its history can be imputed using MCMC. We develop a class of sequential Monte Carlo algorithms that are more generally applicable to sequential network models, and may be of interest in their own right. The model parameters can be recovered from a single graph generated by the model. Applications to data clarify the role of the random walk length as a length scale of interactions within the graph.

1. Introduction. We consider problems in network analysis where the observed data constitutes a single graph. Tools developed for such problems include, for example, graphon models [9, 30, 6, 2, 58, 24], the subfamily of stochastic blockmodels [e.g. 27], preferential attachment graphs [4], interacting particle models [39], and others. In this context, a statistical model is a family $\mathcal{P} = \{P_{\theta}, \theta \in \mathbf{T}\}$ of probability distributions on graphs, and sample data is explained either as a single graph drawn from the model, or as a subgraph of such a graph.

Applied network analysis distinguishes between network formation mechanisms that are *endogenous* (are an outcome of the current structure of the network), and those that are *exogenous* (are driven by external effects), see e.g. [53, 41]. We develop methodology to account for endogenous mechanisms. That necessarily introduces stochastic dependence between existing and newly emerging structure in the network. The technical challenge is to identify models that nonetheless are statistically and computationally tractable.

The approach taken in the following is generative, in the sense that it formulates a model of how a graph grows as a stochastic process. Specifically, the class of models we study generate a graph by inserting one edge at a time: Initialize a graph as a single edge, with its two terminal vertices. For each new edge, select a vertex V in the current graph at random.

- With a fixed probability $\alpha \in (0,1]$, add a new vertex and connect it to V.
- Otherwise, start a random walk at V, and connect its terminal vertex to V.

The result is a graph or multigraph, with a random number of vertices labeled in

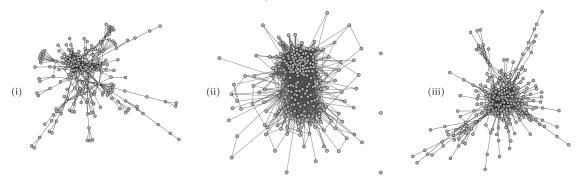
order of occurrence. Generative network models are studied in applied probability [e.g. 22], where they are often motivated by how generative mechanisms determine properties of the graph. Perhaps the best-known examples are preferential attachment graphs, in which a simple generative mechanism (reinforcement based on degree-biased selection of vertices) explains an observable characteristic of networks (power law degrees). For the purposes of statistics, a family of generative distributions is applicable as a model if (i) it can be parametrized in a meaningful way and (ii) if parameter inference from observed data is possible. As the ensuing discussion shows, inference using MCMC techniques is possible for a range of generative models, including the one sketched above.

The endogenous mechanism characterizing the model above is the random walk, which lets vertices connect "through the network". At each step, an endogenous mechanism is chosen with probability $(1-\alpha)$, or an exogenous one with probability α . In contrast to the models listed at the outset, the locations of newly inserted edges thus depend on those of previously inserted ones, and the effect of this dependence is clearly visible in graphs generated by the model (see Figure 1 in Section 2 for examples). The random walk step itself can be regarded as a model of interactions:

- Long walks can connect vertices far apart in the graph. The (expected) length of the walk can hence be regarded as a range scale.
- Where convenient, the walk may be interpreted explicitly, as a process on the network (e.g. users in a social network forming connections through other users). More generally, it biases connections towards vertices reachable along multiple paths.

We show in the following that random walk models can explain a range of graph structures as the outcome of interactions mediated by the network, and are statistically and analytically tractable.

Background. At a conceptual level, the work presented here is motivated by the question of how statistical network models handle stochastic dependence within a network; the discussion in this paragraph is purely heuristic. Consider the link graph of a network, regarded as a system of random variables (representing edges and vertices). Informally, for structure to occur in a network with non-negligible probability, the variables must be dependent. The graphs below are (i) a protein-protein interaction network (see Section 5), and (ii) its reconstruction sampled from a graphon model fitted to (i), and (iii) a reconstruction from the random walk model:



The data set in (i) contains pendants (several degree-1 vertices linked to a single vertex), isolated chains of edges, etc. For these to arise at random requires local dependence between edges on different length scales, and they are conspicuously absent in (ii). That is not a shortcoming of the method used to fit the model, but inherent to graphons per se, since these models constrain edges to be conditionally independent given certain vertex-wise information. If the missing structure is relevant to statistical analysis, its absence constitutes a form of model misspecification. To put the problem into context, it is useful to compare some commonly used models:

- Graphon models (as mentioned above). These have recently received considerable attention in statistics, and include stochastic blockmodels [27], and many models popular in machine learning [see 45].
- Models that randomize a graph to match a given degree sequence, such as the configuration model [22].
- Models describing a formation process, such as preferential attachment (PA) models [4].

All of these models constrain dependence by rendering edges conditionally independent given some latent variable: In a graphon model, this latent variable is a local edge density; in the related model of Caron and Fox [15], a scalar variable associated with each vertex; in recent so-called edge exchangeable models [19, 56, 14], a random measure associated with the edges; in a configuration model, the degree sequence; in PA models, the vertex arrival times and a vector of vertex-specific variables [7]. Some of these models have been noted to be misspecified for network analysis problems. For example:

- In the case of graphon models, various symptoms of this problem have been noted [e.g. 10, 45]: The generated graph is dense; unless it is k-partite or disconnected, the distance between any two vertices in an infinite graph is almost surely 1 or 2; etc. A graphon can encode any fixed pattern on some number n of vertices, but this pattern then occurs on every possible subgraph of size n with fixed probability.
- Configuration models are popular in probability (due to their simplicity), but have limited use in statistics unless the quantity of interest is the degree sequence itself: They are "maximally random" given the degrees, in a manner similar to exponential families being maximally random given a sufficient

statistic, and are thus insensitive to any structure not captured by the degrees. Other models based on degrees (PA models, the model of Caron and Fox [15], so-called rank one edge exchangeable models [33]) are similarly constrained.

In each instance of misspecification listed, the constraints on dependence are culpable. Nonetheless, such constraints are imposed for good reasons. One is tractability: As in any system of multiple random variables, forms of stochastic dependence amenable to mathematical analysis and statistical inference are rare. Another is the basic design principle that a statistical model should be as simple as possible: The presence, not absence, of dependence requires justification.

The approach taken here is to make a modeling assumption on the network formation process: Edges are formed via interactions mediated by the network, in the form of random walks. Consequently, no known form of exchangeability is present in random walk models. Whether that modeling assumption is considered adequate must depend on the problem at hand. A non-exchangeable model is best suited to data for which the order of the edges might be informative, even if it is unknown. This type of problem arises, for example, in genetics and evolutionary biology [e.g. 43]. Conceptually, the random walk models studied in the following allow slightly more intricate forms of stochastic dependence than the models discussed above, without sacrificing applicability.

Article overview. Random walk models are defined in Section 2. They can be chosen to generate either multigraphs or simple graphs, which are sparse in either case. A quantity that plays a key role in both theory and inference is the history of the graph, i.e. the order Π in which edges are inserted. In dynamic networks [e.g. 36, 22], where a graph is observed over time, Π is an observed variable. If only the final graph is observed, Π is latent. Section 3 establishes some theoretical properties:

- If the entire history Π of a multigraph is observed, model parameters can be estimated by maximum likelihood (Section 3.2).
- Under suitable conditions, the limiting degree distribution can be characterized (Theorem 3.3). The generated graphs can exhibit power law properties.
- Conditionally on the times at which vertices are inserted, the normalized degree sequence converges to an almost sure limit. Results of this type are known for preferential attachment models. Each limiting relative degree can be generated marginally by a sampling scheme reminiscent of "stick-breaking". See Theorem 3.4.
- If the length of the random walk tends to infinity, the model converges to a generalization of the preferential attachment model (Proposition 3.5).

If only the final graph is observed, inference is still possible, by treating the history II as a latent variable and imputing it using a sampling algorithm. This problem is of broader interest, since it permits the application of sequential or dynamic network models, including the PA model and many others, to a single observed graph. In Section 4, we show how the graph history can be sampled, under any sequential network model satisfying a Markov and a monotonicity property, using a Sequential Monte Carlo (SMC) algorithm. Using this algorithm, we derive inference algorithms for sequential network models that can be designed as SMC or particle

MCMC methods [3]. In Section 5, we report empirical results and applications to data:

- Applicability of the model is evaluated by performing parameter inference on synthetic data sampled from the model. Parameters indeed can be recovered from a single observed graph.
- The role of the random walk parameter can be understood in more detail by relating it to the mixing time of a simple random walk on the data set; see Section 5.2.
- Comparisons between the random walk model and other network models are given in Section 5.3; we also discuss issues raised by such how comparisons are performed.
- The latent order Π can be related to measures of vertex centrality (Section 5.4).

Data and code are available at https://github.com/ben-br/random_walk_smc.

2. Random walk graph models: Definition. Throughout, g generically denotes a fixed graph, and G a random graph. A random walk on a connected graph g, started at vertex v, is a random sequence (v, V_1, \ldots, V_k) of vertices, such that neighbors in the sequence are connected in g. Figuratively, a walker repeatedly moves along an edge to a randomly selected neighbor, until k edges have been crossed. Edges and vertices may be visited multiple times. The random walk is simple if the next vertex is selected with uniform probability from the neighbors of the current one. The distribution of the terminal vertex V_k of a simple random walk on g, of length k, and starting at v, is denoted SRW(g, v, k). The model considered in the following is, like many sequential network models, most easily specified as an algorithm:

Algorithm 1 (Random walk model on multigraphs).

- Fix $\alpha \in (0,1]$ and a distribution P on \mathbb{N} . The initial graph G_1 consists of a single edge connecting two vertices.
- For t = 2, ..., T, generate G_t from G_{t-1} as follows:
 - (1) Select a vertex V of G_{t-1} at random (see below).
 - (2) With probability α , attach a new vertex to V.
 - (3) Else, draw $K \sim P$ and connect V to $V' \sim SRW(G_{t-1}, V, K)$.

The vertex V in (1) is either sampled uniformly from the current vertex set, or from the **size-biased** (or **degree-biased**) distribution $\mathbb{S}(v) = \deg(v) / \sum_{v' \in \mathcal{V}(g)} \deg(v')$, where $\deg(v)$ is the degree of vertex v in g. In principle, the initial graph G_1 can be chosen as an arbitrary, fixed "seed graph", but we work with a single edge throughout. The random walk models endogenous formation of edges along existing paths in the graph—for illustration, consider a meeting process in a social network, where users meet through one or several acquaintances.

Algorithm 1 generates multigraphs, since the two vertices selected by the random walk may already be connected (resulting in a multi-edge), or may coincide (result-

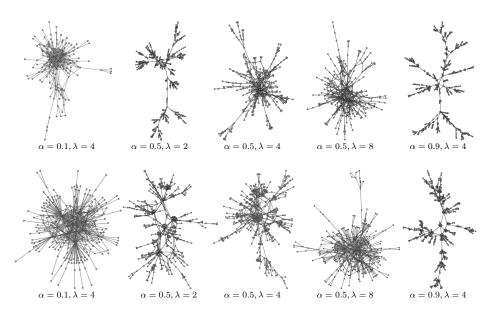


Fig 1. Examples of simple graphs generated by a random walk model: $\mathbf{RW}_{U}(\alpha, Poisson_{+}(\lambda))$ distribution (top row), and by a $\mathbf{RW}_{SB}(\alpha, Poisson_{+}(\lambda))$ distribution (bottom row).

ing in a self-loop). To generate simple graphs instead, step (3) above is replaced by:

(3') Else, draw $K \sim P$ and $V' \sim \text{SRW}(G_{t-1}, V, K)$. Connect V to V' if they are distinct and not connected; else, attach a new vertex to V.

Either sampling scheme defines the law of a sequence $(G_1, G_2, ...)$ of graphs. We denote this law $\mathbf{RW}_{\mathrm{U}}(\alpha, P)$ if the vertex V in (1) is chosen uniformly, or $\mathbf{RW}_{\mathrm{SB}}(\alpha, P)$ in the size-biased case. Each such law is defined both on multigraphs and on simple graphs, depending on which sampling scheme is used.

We usually choose the length of the random walk as a Poisson variable: Denote by $\operatorname{Poisson}_{+}(\lambda)$ the Poisson distribution with parameter λ , shifted by 1, i.e. the law of K+1, where K is Poisson. We write $\operatorname{\mathbf{RW}}(\alpha,\lambda)$ for $\operatorname{\mathbf{RW}}(\alpha,\operatorname{Poisson}_{+}(\lambda))$ where convenient. Examples of graphs generated by this distribution are shown in Figure 1.

3. Model properties. We first observe that graphs generated by the model are sparse by construction. Let $(G_1, \ldots, G_t, \ldots)$ be a graph sequence generated by any **RW** model on simple or multigraphs, with parameter α , where G_1 has a single edge connecting two vertices. Denote by $\mathcal{V}(G_t)$ and $\mathcal{E}(G_t)$ the set of vertices and of edges, respectively, in G_t . For any **RW** model, each vertex is added with one edge and there is a constant positive probability at each step of adding a new vertex, which leads to the following:

OBSERVATION. Graphs generated by the random walk model are sparse: In a sequence $(G_1, G_2, \ldots) \sim \mathbf{RW}(\alpha, P)$, the number of edges grows as $|\mathcal{E}(G_t)| = \Theta(|\mathcal{V}(G_t)|)$.

If the model is run for an infinite number of steps (with $\alpha > 0$), it generates an infinite number of vertices. Sparsity implies this infinite vertex set is not exchangeable. Since vertices inserted earlier have larger expected degree, finite subsequences of vertices are not exchangeable, either.

3.1. Mixed random walks and the graph Laplacian. Most results in the sequel involve the law of a simple random walk. For a walk of fixed length, this law is determined by the graph's Laplacian matrix. If the length is random, one has to mix against its distribution; as we show below, the mixed law of the random walk still has closed form.

Consider an undirected graph G with n vertices, adjacency matrix A and degree matrix $D = \operatorname{diag}(\operatorname{deg}(v_1), \ldots, \operatorname{deg}(v_n))$. The probability that a simple random walk started at a vertex u terminates at v after exactly k steps is the entry (u, v) of the matrix $(D^{-1}A)^k$. If the length of the walk is a random variable K with law P, the marginal probability of reaching v from u is hence

$$\mathbb{P}\{V_{end} = v | V_0 = u, G\} = \left[\sum_k (D^{-1}A)^k P\{K = k\} \right]_{uv} = \left[\mathbb{E}_P \left[\left(D^{-1}A \right)^k \right] \right]_{uv}.$$
(1)

A useful way to represent the information in $D^{-1}A$ is as the matrix

$$\mathbf{L} := D^{1/2}(\mathbb{I}_n - D^{-1}A)D^{-1/2} \quad \text{with } \mathbb{I}_n := \text{identity matrix} , \qquad (2)$$

known as the **normalized graph Laplacian** [e.g., 18]. Letting the probability generating function (p.g.f.) of K be $H_P(z) = \mathbb{E}_P[z^K]$, the law of a random walk of random length is obtained as follows:

PROPOSITION 3.1. Let g be a connected, undirected graph on n vertices, and let K have law P with p.g.f. $H_P(z)$. Let $(\sigma_i)_{i=1}^n$ be the eigenvalues, and $(\psi_i)_{i=1}^n$ the eigenvectors, of \mathbf{L} . Then for a simple random walk (V_0, \ldots, V_K) of random length K on g,

$$\mathbb{P}\{V_{end} = v | V_0 = u, g\} = \left[D^{-1/2} \mathcal{K}_P D^{1/2}\right]_{uv} \quad with \quad \mathcal{K}_P := \sum_{i=1}^n H_P (1 - \sigma_i) \psi_i \psi_i'.$$
(3)

For a Poisson₊(λ) length, the result specializes to $\mathcal{K}_{\lambda+} := (\mathbb{I}_n - \mathbf{L})e^{-\lambda \mathbf{L}}$. If overdispersion is a concern, one can replace the Poisson by a negative binomial distribution with parameters r and p, again shifted by one to the positive integers, and denoted NB₊(r, p). In that case, one obtains $\mathcal{K}_{r,p+} := (\mathbb{I}_n - \mathbf{L})(\mathbb{I}_n + \frac{p}{1-p}\mathbf{L})^{-r}$. These matrices arise in other contexts: The **heat kernel** $\mathcal{K}_{\lambda} = e^{-\lambda \mathbf{L}}$ and the **regularized Laplacian kernel** $\mathcal{K}_{r,p} = (\mathbb{I}_n + \frac{p}{1-p}\mathbf{L})^{-r}$ have applications in collaborative filtering, semi-supervised learning and manifold learning [51, 38]. Both act as smoothing operators on functions defined on the vertex set, by damping the eigenvalue spectrum [51, 54]. The expected length of the random walk can be interpreted as a length scale (see Section 5), and a similar idea was previously used by Pons and Latapy [49] to define a distance between vertices of a graph: if the distribution over the terminal vertex of a random walk of (fixed) length k started from vertex u is close to that started from vertex v, then u and v are "close." It can be regularized by mixing the walk length against a Poisson distribution, as suggested in Pons and Latapy [49, Sec. 3.4]. We note that, using Proposition 3.1 above, the Pons–Latapy metric can be regularized more generally by an arbitrary walk length distribution.

3.2. Maximum likelihood estimation for fully observed sequences. In the special case of "dynamic" multigraphs, where the entire history is observed, model parameters can be estimated by maximum likelihood. Let (v_s, v'_s) be the vertices connected in step s, and $B_s := \mathbb{1}\{\min\{\deg_{s-1}(v_s), \deg_{s-1}(v'_s)\} = 0\}$. That is, the edge was generated by step (2) of the sampling scheme if and only if $B_s = 1$. Define

$$Q_s^{\lambda} := D_s^{-1/2} \mathcal{K}_{\lambda +, s} D_s^{1/2} , \qquad (4)$$

and denote by $\bar{d}_s(v)$ the relative degree of vertex v in G_s .

PROPOSITION 3.2. Let $(G_1, \ldots, G_t) \sim \mathbf{RW}_{SB}(\alpha, \operatorname{Poisson}_+(\lambda))$ be a random multigraph sequence, where G_1 has a single edge connecting two vertices. Then

$$\hat{\alpha}_t := \frac{N_t - 2}{t - 1} \quad and \quad \hat{\lambda}_t := \arg\max_{\lambda \ge 0} \prod_{s = 2}^t \left([Q_{s-1}^{\lambda}]_{v_s v_s'} \bar{d}_{s-1}(v_s) + [Q_{s-1}^{\lambda}]_{v_s' v_s} \bar{d}_{s-1}(v_s') \right)^{1 - B_s}$$

are maximum likelihood estimators of α and λ , respectively.

The same holds for $\mathbf{RW}_{\mathsf{U}}(\alpha, \mathrm{Poisson}_{+}(\lambda))$, with $1/N_{s-1}$ substituted for $\bar{d}_{s-1}(v_s)$ in $\hat{\lambda}_t$. To change the walk length distribution, one must replace $\mathcal{K}_{\lambda+}$ in (4) with the appropriate matrix from (3). For simple graphs, maximum likelihood estimation is still possible in principle, but more complicated since the effects of α and λ are no longer independent. This manifests in step (3') in Section 2, where the probability of generating an additional vertex depends on the outcome of the random walk. Conceptually, it is due to the fact that a simple graph censors evidence of repeatedly connecting two vertices.

3.3. Asymptotic degree properties. A property of network models thoroughly studied in the theoretical literature is how vertex degrees behave as the graph grows large. For PA graphs, limiting degree distributions can be determined analytically [22]. Our next results describe analogous properties for random walk models. In the proofs, effects of the random walk are mitigated by using invariance of the degree-biased distribution under \mathcal{K}_P in (3) to reduce to techniques developed for preferential attachment.

Consider a \mathbf{RW}_{SB} random multigraph, and let p_d be the probability that a vertex sampled uniformly at random has degree d. The proof of the next result shows that,

if the average probability (over vertices) of inserting a self-loop vanishes for large t, then

$$p_d = \rho \frac{\Gamma(d)\Gamma(1+\rho)}{\Gamma(d+1+\rho)}$$
 where $\rho := 1 + \frac{\alpha}{2-\alpha}$. (5)

as $t \to \infty$. This is the **Yule–Simon distribution** with parameter ρ [e.g. 22]. To state the result, let $\mathcal{V}_{d,t}$ be the set of vertices in G_t with degree d, and $m_{d,t} = |\mathcal{V}_{d,t}|$.

THEOREM 3.3 (Degree distribution). Let a sequence of multigraphs $(G_1, G_2, ...)$ have law $\mathbf{RW}_{SB}(\alpha, P)$, for some distribution P on \mathbb{N} , such that for each $d \in \mathbb{N}$,

$$\frac{1}{m_{d,t}} \sum_{v \in \mathcal{V}_{d,t}} P(V_{end} = v | V_0 = v, G_t) = o(1) \quad as \ t \to \infty.$$
 (6)

Then the scaled number of vertices in G_t with degree d follows a power law in d with exponent $1 + \rho$. In particular, $\frac{m_{d,t}}{\alpha t} \to p_d$ in probability, for all $d \in \mathbb{N}_+$ as $t \to \infty$.

Condition (6) controls the number of self-loops, by requiring that the probability of a random walk ending where it starts vanishes for $t \to \infty$, separately for each degree d. Simulations indicate that it holds for many walk length distributions, including Poisson.

Denote by $\mathbf{deg}_t := (\deg_t(v_1), \deg_t(v_2), \dots)$ the \mathbf{degree} sequence, where v_j is the j-th vertex to appear in the graph sequence. For PA models, the limiting sequence \mathbf{deg}_{∞} can be studied analytically [see e.g. 22]. It is closely related to a Pólya urn, and like the limit of an urn, \mathbf{deg}_{∞} is itself a random variable. Informally, edges created early have sufficiently strong influence on later edges that randomness does not average out asymptotically. The joint law of \mathbf{deg}_{∞} can be obtained explicitly [42, 46]. In some cases, it also admits constructive representations: Using only sequences of independent elementary random variables, one can generate a random sequence whose joint distributions are identical to those of the limiting degree sequence [42, 32, 7]. Such representations are closely related to "stick-breaking constructions" [e.g. 47].

The next result similarly describes the limiting degree sequence \deg_{∞} of the $\mathbf{RW}_{\mathrm{SB}}$ model. The relevant technical tool is to condition on the order in which edges occur: For a graph sequence (G_1, G_2, \ldots) , denote by S_j the time index at which vertex v_j is inserted in the model (that is, G_{S_j} is the first graph containing v_j), and let $S_{1:r} := (S_1, \ldots, S_r)$. Let Σ_{β} be a positive stable random variable with index $\beta \in (0,1)$, with Laplace transform $\mathbb{E}[e^{-t\Sigma_{\beta}}] = e^{-t^{\beta}}$, and f_{β} its density. Define $\Sigma_{\beta,\theta}$, for $\theta > -\beta$, as a random variable with the polynomially tilted density $f_{\beta,\theta}(s) \propto s^{-\theta} f_{\beta}(s)$. The variable $M_{\beta,\theta} := \Sigma_{\beta,\theta}^{-\beta}$ is said to have **generalized Mittag–Leffler distribution** [47, 32].

THEOREM 3.4 (Degree sequence). Let a sequence of multigraphs $(G_1, G_2, ...)$ have law $\mathbf{RW}_{SB}(\alpha, P)$, for some distribution P on \mathbb{N} . Conditionally on $(S_1, S_2, ...)$,

the scaled degree sequence converges jointly to a random limit: For each $r \in \mathbb{N}_+$,

$$t^{-1/\rho}(\deg_t(v_1), \deg_t(v_2), \dots, \deg_t(v_r)) \mid S_{1:r} \xrightarrow{t \to \infty} (\xi_1, \xi_2, \dots, \xi_r) \mid S_{1:r}$$
 (7)

almost surely. Each limiting conditional law $\mathcal{L}(\xi_j \mid S_j)$, for $j \geq 1$, can be represented constructively: Let $M_j \sim \text{Mittag-Leffler}\left(\rho^{-1}, S_j - 1\right)$, $B_j \sim \text{Beta}\left(1, \rho(S_j - 1)\right)$, and $\psi_j \sim \text{Beta}\left(S_j, S_{j+1} - S_j\right)$ be conditionally independent given S_j . Then for $1 \leq i < j$

$$\xi_{j}|S_{j} \stackrel{d}{=} M_{j} \cdot B_{j}|S_{j} \stackrel{d}{=} \xi_{i} \prod_{k=i}^{j-1} \psi_{k}^{1/\rho} |S_{i:j}|.$$
 (8)

Each marginal law $\mathcal{L}(\xi_i)$ is uniquely determined by the sequence of moments

$$\mathbb{E}\left[\xi_{j}^{k}\right] = \frac{\Gamma(k+1)\Gamma(j-1)}{\Gamma(j-1+\frac{k}{\rho})} \alpha^{\frac{k}{\rho}} {}_{2}F_{1}\left(1+\frac{k}{\rho},\frac{k}{\rho};j-1+\frac{k}{\rho};1-\alpha\right) \tag{9}$$

where $_2F_1(a,b;c;z)$ is the ordinary hypergeometric function.

We note the moment $\mathbb{E}\left[\xi_{j}^{k}\right]$ scales as $\Gamma(k+1)\alpha^{\frac{k}{\rho}}j^{-\frac{k}{\rho}}\cdot(1+O(j^{-1}))$ for $j\to\infty$. The simple constructive representation (8) seems only to exist marginally, in contrast to the PA model, where a recursive analogue of (8) holds even jointly [32].

3.4. Relation to preferential attachment and other models. Aiello et al. [1] introduced a generalization of preferential attachment graphs: Fix $\alpha \in (0,1]$. At each step, select two vertices V,V' independently from the degree-biased distribution. With probability α , insert a new vertex and connect it to V; otherwise, connect V and V'. The model is denoted $\mathbf{ACL}(\alpha)$, and can be regarded as a natural extension of Yule–Simon processes from sequences to graphs.

PROPOSITION 3.5. The limit in distribution $\mathbf{RW}_{SB}(\alpha, \infty) := \lim_{\lambda \to \infty} \mathbf{RW}_{SB}(\alpha, \lambda)$ exists for every α , and $\mathbf{RW}_{SB}(\alpha, \infty) = \mathbf{ACL}(\alpha)$ if both models start with the same seed graph.

This is of course due to the fact that, as $\lambda \to \infty$, the terminal vertex of simple random walk has law approaching the degree-biased distribution. The same is true for any random walk model in the limit where the walk length distribution becomes degenerate at ∞ (analogously to $\lambda \to \infty$). For $\alpha = 1$ (and any λ), both the random walk model and the $\mathbf{ACL}(\alpha)$ model coincide with the Barabási–Albert preferential attachment tree.

Random walk models generate networks one edge at a time; this specification of a graph may be viewed as a sequence of edges. Recent work on so-called edge exchangeable graphs [19, 56, 14, 33] define network models in terms of an exchangeable sequence of edges. Edges in random walk models are not exchangeable. The limiting **ACL** model, however, and a subclass of edge exchangeable graphs both belong to a larger class of models whose distributions are characterized by the arrival times of new vertices [7].

3.5. Covariate information. We briefly mention two possible extensions not further considered in our discussion. Nodal covariates \mathbf{X} represent exogenous effects on edge formation; when available, they can be incorporated by biasing the probability of a random walk started at u to end at v by a function of the covariate values at u and v. A simple way to do so is via a kernel matrix $\mathcal{K}_{\mathbf{X}}$, where $[\mathcal{K}_{\mathbf{X}}]_{uv}$ expresses a suitable notion of similarity between u and v, based on \mathbf{X} . To this end, let $\mathcal{K}_{P+\mathbf{X}} := \mathcal{K}_P + \mathcal{K}_{\mathbf{X}}$. Define $\deg_{P+\mathbf{X}}(u) = \sum_v [\mathcal{K}_{P+\mathbf{X}}]_{uv}$, and let $D_{P+\mathbf{X}}$ be the diagonal matrix with entries $[D_{P+\mathbf{X}}]_{uu} = \deg_{P+\mathbf{X}}(u)$. The probability of a new edge between u and v is then

$$\mathbb{P}\{(u,v)|V_0=u,g\}=[D_{P+\mathbf{X}}^{-1}\mathcal{K}_{P+\mathbf{X}}]_{uv}.$$

For example, the kernel can be chosen to express homophily, the tendency of similar vertices to form edges [e.g. 29]. Similarly, one can bias the "popularity" of a vertex by adding a scalar offset to each degree that depends on covariates: Choose functions f_i with range $(-1, \infty)$ (to ensure the biased degrees remain positive), and replace matrices in (1) by $D' = \operatorname{diag}(\operatorname{deg}(v_1) + f_1(\mathbf{X}), \dots, \operatorname{deg}(v_n) + f_n(\mathbf{X}))$, and $A'_{i,j} = A_{i,j}(1 + f_i/\operatorname{deg}(v_i))$. The inference methods developed below remain applicable, provided the functions f_i depend only on exogenous covariates, not on the graph. Temporal covariates, such as age, can also be incorporated into the order in which vertices appear.

4. Particle methods for sequential network models. Our modeling approach is to use a suitably parametrized sequential random graph as a statistical model. One could similarly use a preferential attachment graph, or some other sequential model considered more appropriate for a given task. The approach poses an inference problem: A sequential network model is assumed, but only the final graph G_T generated by the model is observed, as opposed to the entire history $G_{1:T} := (G_1, \ldots, G_T)$ of the generative process. This section develops Markov chain Monte Carlo methods for inference in sequential random graph models, and in random graph models in particular.

Given the choice of G_1 —typically a graph consisting of a single edge—T is always uniquely determined by the number of edges in the observed graph, since each step of the generative process inserts exactly one edge. The methods developed here assume a Bayesian setup, with a prior distribution $\mathcal{L}(\theta)$ on the model parameter θ , where $\mathcal{L}(\bullet)$ generically denotes the law of a random variable. They sample the posterior distribution $\mathcal{L}(\theta|G_T)$, and are applicable to sequential network models satisfying two properties:

- (P1) The sequence (G_1, \ldots, G_T) of graphs generated by the models forms a Markov chain on the set of finite graphs: $G_{t+1} \perp \!\!\! \perp (G_1, \ldots, G_{t-1}) \mid G_t$, for each t < T.
- (P2) The sequence is strictly increasing, in the sense that $G_t \subsetneq G_{t+1}$ almost surely.

These hold for the random walk models, but also for many other network formation models, such as preferential attachment graphs, fitness models, and vertex copying models [e.g. 44, 27]. Despite the attention these models have received in the literature, little work exists on inference (see Section 4.5 for references).

If only a single graph G_T is observed, inference requires that the unobserved history is integrated out. The result is a likelihood of the form

$$p_{\theta}(G_T \mid G_1) = \int p_{\theta}(G_T, G_{2:(T-1)} \mid G_1) dG_{2:(T-1)}.$$
 (10)

Since the variables G_t take values in large combinatorial sets, the integral amounts to a combinatorial sum that is typically intractable. The strategy is to approximate the integral with a sampler that imputes the unobserved graph sequence, noting that only valid sequences which lead to G_T will have non-zero likelihood (10). The sequential nature of the models makes SMC and particle methods the tools of choice.

4.1. Basic SMC. We briefly recall SMC algorithms: The canonical application is a state space model. Observed is a sequence $X_{1:T} = (X_1, \ldots, X_T)$. The model explains the sequence using an unobserved sequence of latent states $Z_{1:T}$, and defines three quantities: (1) A Markov kernel $q_{\theta}^t(\bullet \mid Z_{t-1})$ that models transitions between latent states. (2) An emission distribution p_{θ}^t that explains each observation as $X_t \sim p_{\theta}^t(\bullet \mid Z_t)$. (3) A vector θ collecting the model parameters. In the simplest case, θ is fixed. The inference target is then the posterior distribution $\mathcal{L}_{\theta}(Z_{1:T} \mid X_{1:T})$ of the latent state sequence.

A SMC algorithm generates some number $N \in \mathbb{N}$ of state sequences $Z_{1:T}^1, \ldots, Z_{1:T}^N$, and then approximates the posterior as a sample average over these sequences, weighted by their respective likelihoods. The imputed states $Z_{1:t}^i$ are called **particles**. Since the sequence of latent states is Markov, particles can be generated sequentially as $Z_t \sim q_\theta^t(Z_t|Z_{t-1})$. In cases where sampling from q_θ^t is not tractable or desirable, q_θ^t it is additionally approximated by a simpler proposal kernel r_θ^t . The likelihood, and the accuracy of approximation of q_θ^t by r_θ^t , are taken into account by computing normalized weights

$$w_t^i := \frac{\tilde{w}_t^i}{\sum_{i=1}^N \tilde{w}_t^j} \quad \text{where} \quad \tilde{w}_t^i = p_{\theta}^t(X_t | Z_t^i) \cdot \frac{q_{\theta}^t(Z_t^i \mid Z_{t-1}^i)}{r_{\theta}^t(Z_t^i \mid Z_{t-1}^i)} \,. \tag{11}$$

In step t, SMC generates particles Z_t^i by first resampling from the previous particles $(Z_{1:t-1}^i)_i$ with probability proportional to their weights:

$$Z_{1:t}^i = (Z_{1:t-1}^{A_t^i}, Z_t^i) \qquad \text{where} \quad Z_t^i \sim r_\theta^t(\bullet \mid Z_{t-1}^{A_t^i}) \text{ and } A_t^i \sim \text{Multinomial}(N, (w_{t-1}^i)_{i=1}^N) \ .$$

Resampling a final time after the T-th step yields a complete array $(Z_{1:T}^i)_i$, with which the posterior is approximated as the average $\mathcal{L}_{\theta}(dz_{1:T} \mid X_{1:T}) \approx \frac{1}{N} \sum_{i=1}^{N} \delta_{Z_{1:T}^i}(dz_{1:T})$. Alternatively, the final resampling step can be omitted, in which case the posterior is approximated with a weighted average. Either approximation is asymptotically unbiased as $N \to \infty$. See Doucet and Johansen [21] for a thorough review.

4.2. SMC algorithms for graph bridges. Consider a sequential network model satisfying properties (P1) and (P2) above, with model parameters θ . For now, θ is fixed, and the objective is to reconstruct the graph sequence $G_{1:T}$ from its observed

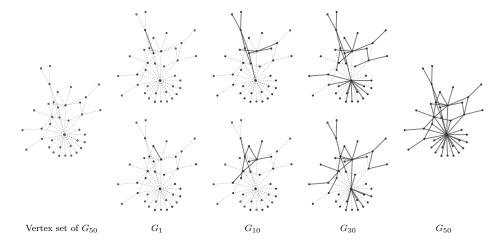


FIG 2. Two graph bridges generated by Algorithm 2: A graph G_{50} is drawn from a $\mathbf{RW}_{\mathrm{U}}(\alpha, P)$ model, and two graph bridges $G_{1:50}$ are sampled conditionally on the fixed input G_{50} . Shown are the graphs G_{1} , G_{10} and G_{30} of each bridge.

final graph G_T and a fixed initial graph G_1 , i.e. the relevant posterior distribution is $\mathcal{L}_{\theta}(G_{1:T} \mid G_T, G_1)$. By the Markov property (P1), each step in the process is governed by a Markov kernel

$$q_{\theta}^{t}(g \mid g') := P(G_{t} = g \mid G_{t-1} = g')$$
.

The task of a sampler is hence to impute the conditional sequence $G_{2:(T-1)} \mid G_1, G_T$, which is a stochastic process conditioned on its initial and terminal point, also known as a **bridge**. Compared to the SMC sampling algorithm for state space models, the unobserved sequence G_2, \ldots, G_{T-1} takes the role of the hidden states $z_{1:T}$, whereas G_1 and the single observed graph G_T replace the observed sequence $x_{1:T}$. The emission likelihood $p_{\theta}^t(x_t|z_t)$ is replaced by a bridge likelihood, of G_T given a graph G_t .

The relevant likelihood functions, however, are themselves intractable: If g_s is a fixed graph at index s in the sequence, the probability of observing g_t at a later point t > s is

$$p_{\theta}^{t,s}(g_t|g_s) := \int \left(\prod_{i=s}^{t-1} q_{\theta}^{i+1}(g_{i+1}|g_i)\right) dg_{s+1} \cdots dg_{t-1}$$
 whenever $t > s$.

For a candidate graph G_t generated by the sampler, the likelihood under observation G_T is the **bridge likelihood** $L^t_{\theta}(G_t) := p_{\theta}^{T,t}(G_T|G_t)$. This likelihood is intractable unless t = T - 1; indeed, for t = 1, it is precisely the integral (10) we set out to approximate.

A sequence $G_{1:T}$ satisfying (P2) is equivalent to an enumeration of the T edges of G_T in order of occurrence. Let π be a permutation of $\{1, \ldots, T\}$, i.e. an ordered

list containing each element of the set exactly once, and

 $\pi_t(G_T) := \text{graph obtained by deleting all edges of } G_T \text{ not in } \pi_t, \text{ and isolated vertices.}$

A random sequence $G_{1:T}$ can then be specified as a pair (Π, G_T) , for a random permutation Π of the edges in G_T , with $G_t = \Pi_t(G_T)$. Given G_T , not every permutation π is a valid candidate value for the unobserved order: π must describe a sequence of steps of non-zero probability from the initial graph to G_T , and we hence have to require

$$L_{\theta}^{t}(\pi_{t}(G_{T})) > 0 \quad \text{for all } t \leq T .$$
 (12)

If so, we call π feasible for G_T . For G_T given and $G_t = \Pi_t(G_T)$, we use G_t and Π_t interchangeably. The target distribution of the SMC bridge sampler at step t is then

$$\gamma_{\theta}(t) := L_{\theta}^{t}(\Pi_{t})P(\Pi_{t}) = L_{\theta}^{t}(\Pi_{t}) \prod_{s=1}^{t-1} q_{\theta}^{s+1}(\Pi_{s+1} \mid \Pi_{s}) , \qquad (13)$$

which satisfies the recursion

$$\gamma_{\theta}(t) = \begin{cases} \frac{L_{\theta}^{t}(\Pi_{t})}{L_{\theta}^{t-1}(\Pi_{t-1})} q_{\theta}^{t}(\Pi_{t}|\Pi_{t-1}) \gamma_{\theta}(t-1) & \text{if } \Pi_{t} \text{ is feasible} \\ 0 & \text{otherwise} \end{cases}.$$

The intractable part is the bridge likelihood ratio $L_{\theta}^{t}/L_{\theta}^{t-1}$. Define

$$h_t(\Pi_t) := \begin{cases} \mathbb{1}\{L_\theta^t(\Pi_t) > 0\} & \text{for all } t < T - 1\\ L_\theta^t(\Pi_t) & \text{for } t = T - 1 \end{cases}.$$

As Proposition 4.1 below shows, the apparently crude approximation $L_{\theta}^{t} \approx h_{t}$ still produces asymptotically unbiased samples from the posterior $\mathcal{L}_{\theta}(G_{1:T} \mid G_{T}, G_{1})$; this is based on methodology developed in [20] for bridges in continuous state spaces. If Π_{t} is feasible, substituting h_{t} into (13) yields the surrogate recursion

$$\gamma_{\theta}(t) = \frac{q_{\theta}^{t}(\Pi_{t} \mid \Pi_{t-1})}{r_{\theta}^{t}(\Pi_{t} \mid \Pi_{t-1})} \gamma_{\theta}(t-1) \quad \text{for} \quad t < T-1.$$

The proposal kernel r_{θ}^{t} is hence chosen as the truncation of q_{θ}^{t} to feasible permutations,

$$r_{\theta}^{t}(\Pi_{t} \mid \Pi_{t-1}) := \frac{\mathbb{1}\{L_{\theta}^{t}(\Pi_{t}) > 0\}q_{\theta}^{t}(\Pi_{t} \mid \Pi_{t-1})}{\tau_{\theta}^{t}(\Pi_{t-1})} \quad \text{with} \quad \tau_{\theta}^{t} := \sum_{\pi_{t}: L_{\theta}^{t}(\pi_{t}) > 0} q_{\theta}^{t}(\pi_{t} \mid \Pi_{t-1}) .$$

$$\tag{14}$$

For particles $G_t^i = \Pi_t^i(G_T)$, the unnormalized SMC weights (11) are

$$\tilde{w}_{t}^{i} = \begin{cases} \tau_{\theta}^{t}(\Pi_{t-1}^{i}) & \text{if } t < T - 1\\ q_{\theta}^{t}(\Pi \mid \Pi_{T-1}^{i}) \ \tau_{\theta}^{T-1}(\Pi_{T-2}^{i}) & \text{if } t = T - 1 \end{cases}$$
 (15)

The sampling algorithm then generates a graph bridge as follows:

Algorithm 2 (Bridge sampling).

- Initialize $G_1^i := G_1$, $\Pi_1^i \sim \text{Uniform}\{1,\ldots,T\}$, and $w_1^i := 1/N$ for each i < N.
- For $t = 2, \ldots, T 1$, iterate:
 - Resample indices $A_t^i \sim \text{Multinomial}(N, (w_{t-1}^i)_i)$.
 - Draw $\Pi_t^i \sim r_\theta^t(\bullet \mid \Pi_{t-1}^{A_t^i})$ as in (14) for each i.
 - Compute weights as in (15) and normalize to obtain w_t^i .
- Resample N complete sequences $G_{1:T}^i = \Pi^i \sim \text{Multinomial}(N, (w_{T-1}^i)_i)$.

See Figure 2 for an illustration. Computing $h_t(\Pi_t)$ and $\tau_t^t(\Pi_{t-1})$ is simplified by the constraints on Π : Given Π_{t-1} , the requirement that Π_t must again be a restriction of a permutation Π implies $\Pi_t = (\Pi_{t-1}, s_t)$, for some $s_t \in \{1, \ldots, T\} \setminus \Pi_{t-1}$. Within this set, the s_t for which Π_t is feasible are simply those edges in G_T connected to $\Pi_{t-1}(G_T)$.

PROPOSITION 4.1. Let q_t^t , for $t=1,\ldots,T$, be the Markov kernels defining a sequential network model that satisfies conditions (P1) and (P2). Given an observation G_T , Algorithm 2 produces samples that are asymptotically unbiased as $N \to \infty$: For any bounded function f on graph sequences, $\frac{1}{N} \sum_{i=1}^{N} f(G_{1:T}^i) \to \mathbb{E}[f(G_{1:T}) \mid G_T, G_1]$ in probability as $N \to \infty$, where the expectation is evaluated with respect to the model posterior.

The particle MCMC methods of the next section will require an unbiased estimate of the bridge likelihood, $L^1_{\theta}(G_1)$, which we state in the following:

PROPOSITION 4.2. Let q_{θ}^t , for t = 1, ..., T, be the Markov kernels defining a sequential network model that satisfies conditions (P1) and (P2), and let r_{θ}^t be the corresponding proposal kernels. Given an observation G_T and a fixed G_1 , the bridge likelihood estimator

$$\hat{L}_{\theta}^{1} := \prod_{t=2}^{T-1} \left[\left(\sum_{i=1}^{N} \frac{\tilde{w}_{t}^{i}}{N} \right) \left(\frac{\sum_{i=1}^{N} h_{t-1} (G_{T} \mid G_{t-1}^{i}) \tilde{w}_{t-1}^{i}}{\sum_{i=1}^{N} \tilde{w}_{t-1}^{i}} \right) \right] . \tag{16}$$

is positive and unbiased: $\hat{L}_{\theta}^1 > 0$ and $\mathbb{E}[\hat{L}_{\theta}^1] = L_{\theta}^1(G_1) = p_{\theta}(G_T \mid G_1)$, for any $N \geq 1$.

Variance reduction. If estimates exhibit high variance, it is straightforward to modify Algorithm 2 to use adaptive resampling [see 20], and to replace multinomial resampling above by residual or stratified resampling [21]. A variance reduction technique due to Fearnhead and Clifford [23] takes advantage of the discrete state space by enumerating possible states Π^i_{t+1} given the current state Π^i_t , creating N' > N "virtual" particles before down-sampling to propagate N particles. Finally, if a given model admits a more bespoke approximation h_t to the bridge likelihood, this approximation can be substituted for h_t , following Del Moral and Murray [20]. In this case, some of the equations above require minor modifications.

4.3. Parameter inference. Algorithm 2 generates a history of a graph under a model with fixed parameter vector θ . For parameter inference, the parameters are treated as a random variable Θ , with prior distribution $\mathcal{L}(\Theta)$, and the task is to generate samples from the joint posterior $\mathcal{L}(\Theta, G_{1:T}|G_1, G_T)$. The sample space of the SMC sampler above is thus extended by the domain of Θ . The bridge likelihood $L_{\Theta}^1(G_1)$ is a marginal likelihood that naturally leads to particle MCMC methods [3], which use SMC to compute an unbiased estimate \hat{L}_{Θ}^1 . Substituting into the Metropolis–Hastings acceptance ratio of a proposal $\tilde{\Theta}$ from a (yet to be specified) proposal distribution \tilde{q} yields

$$\mathbb{P}\{ \text{ accept } \tilde{\Theta} \} = \frac{\hat{L}_{\tilde{\Theta}}^{1} \cdot \pi(\tilde{\Theta})}{\hat{L}_{\Theta}^{1} \cdot \pi(\Theta)} \cdot \frac{\tilde{q}(\Theta \mid \tilde{\Theta})}{\tilde{q}(\tilde{\Theta} \mid \Theta)}.$$
 (17)

By Proposition 4.2, a positive unbiased estimate of the bridge likelihood is given by (16); with (17), we obtain a particle marginal Metropolis–Hastings (PMMH) sampler:

Algorithm 3.

- Initialize $\Theta^0 \sim \pi$.
- For $j = 1, \ldots, J$ iterate:
 - 1. Draw candidate a value $\tilde{\Theta} \sim \tilde{q}(\bullet \mid \Theta^{j-1})$.
 - 2. Run Algorithm 2 with parameter $\tilde{\Theta}$ to compute \hat{L}^1_{Θ} as in (16).
 - 3. Accept $\tilde{\Theta}$ with probability (17) and set $\Theta^j := \tilde{\Theta}$; else set $\Theta^j := \Theta^{j-1}$.
 - 4. If $\tilde{\Theta}$ is accepted, select a single graph sequence $G_{1:T}^j$ by resampling from the particles output by Algorithm 2; else set $G_{1:T}^j = G_{1:T}^{j-1}$.
- Output the sequence $(\Theta^1, G^1_{1:T}), \dots, (\Theta^J, G^J_{1:T})$.

The algorithm asymptotically samples the joint posterior $\mathcal{L}(\Theta, G_{1:T} \mid G_1, G_T)$, or the marginal posterior $\mathcal{L}(\Theta \mid G_1, G_T)$ if the output of step (d) is omitted:

PROPOSITION 4.3. If the proposal density $\tilde{q}(\bullet|\bullet)$ is chosen such that the Metropolis–Hastings sampler defined by (17) is irreducible and aperiodic, Algorithm 3 is a PMMH sampler. The marginal distributions $\mathcal{L}(\Theta^j, G^j_{1:T})$ of its output sequence satisfy

$$\|\mathcal{L}(\Theta^j, G_{1:T}^j) - \pi(\bullet \mid G_T, G_1)\|_{\text{TV}} \xrightarrow{j \to \infty} 0.$$
 (18)

This is true regardless of the sample size N generated by Algorithm 2 in step (b).

4.4. Particle Gibbs for random walk models. The computational cost of Algorithm 3 stems mostly from rejections in (c), each of which requires an additional execution of (b). This can be addressed by turning the algorithm into a Gibbs sampler, which eliminates both rejections and the need for a proposal kernel \tilde{q} . The result is a particle Gibbs (PG) sampler [3]. Such an algorithm is described below, now specifically for the random walk model.

For a $\mathbf{RW}(\alpha, \operatorname{Poisson}_+(\lambda))$ model, the parameter takes the form $\Theta = (\alpha, \lambda)$, and we fix a beta distribution $P_{[\alpha]}$ as prior for α , and a gamma prior $P_{[\lambda]}$ for λ . To sample a sequence G_1, \ldots, G_T from the model, one can generate two i.i.d. sequences, $\mathbf{B} = (B_1, \ldots, B_T)$ of Bernoulli(α) variables, and $\mathbf{K} = (K_1, \ldots, K_T)$ of Poisson₊(λ) variables. In step t, a new edge is inserted if $B_t = 1$; otherwise, two vertices are connected by a random walk of length K_t . As shown in Appendix B, the entries B_t , K_t and the model parameters can be integrated out of the kernel. \mathbf{B} and \mathbf{K} can hence be sampled separately from the SMC steps, rather than inside Algorithm 2, which improves exploration.

In its jth iteration, the algorithm updates **B** and **K** by looping over the indices $t \leq T$ of $G_{1:T}$. Since Gibbs samplers condition on every update immediately, vectors maintained by the sampler are of the form

$$\mathbf{B}_{-t}^j := (B_1^{j+1}, \dots, B_{t-1}^{j+1}, B_t^j, \dots, B_T^j) \quad \text{ and } \quad \mathbf{K}_{-t}^j := (K_1^{j+1}, \dots, K_{t-1}^{j+1}, K_t^j, \dots, K_T^j)$$

The posterior predictive distributions of B_t^{j+1} and K_t^{j+1} given these vectors can be obtained in closed form (see Appendix B). We abuse notation and let the index j=0 refer to the prior predictive distribution, i.e. we write $\mathcal{L}(\mathbf{B}^1|\mathbf{B}^0,G_{1:T}^0):=\int \mathcal{L}(\mathbf{B}^1\mid\alpha)P_{\alpha}(d\alpha)$, and similarly for $\mathcal{L}(\mathbf{K}^1\mid\mathbf{K}^0,G_{1:T}^0)$.

Algorithm 4 (Particle Gibbs sampling for $\mathbf{RW}(\alpha, \text{Poisson}_{+}(\lambda))$ models.).

- For j = 0, ..., J:
 - 1. Draw $(\mathbf{B}^{j+1}, \mathbf{K}^{j+1}) \sim \mathcal{L}(\mathbf{B}^{j+1}, \mathbf{K}^{j+1} \mid \mathbf{B}^{j}, \mathbf{K}^{j}, G_{1:T}^{j}).$
 - 2. Using Algorithm 2, with $q_{\alpha,\lambda}^t(\:\bullet\:|\:G_{t-1}^j,\mathbf{B}_{-t}^{j+1},\mathbf{K}_{-t}^{j+1})$ and $N\geq 2$, update $G_{1:T}^{j+1}$ and $A_{2:T}^{j+1}$. At each step t, substitute the previous iteration's bridge $G_{1:t}^j$ for the particle with index A_t^j (see below).
 - 3. Draw $\alpha^{j+1} \mid \mathbf{B}^{j+1}$ and $\lambda^{j+1} \mid \mathbf{K}^{j+1}$ from their conjugate posteriors.
- Output the sequence $(G_{1:T}^1, \alpha^1, \lambda^1), \ldots, (G_{1:T}^J, \alpha^J, \lambda^J)$.

The algorithm constitutes a blocked Gibbs sampler. The parameter values α^j and λ^j generated in (c) are not used in the execution of the sampler; they only serve as output. Step (b) is a **conditional SMC** step [see 3] that conditions on $G_{1:T}^j$, and makes it a valid Gibbs sampler.

COROLLARY 4.3.1. Algorithm 4 is a valid particle Gibbs sampler. For any $N \geq 2$, it generates a sequence $(G_{1:T}^j, \alpha^j, \lambda^j)_j$ whose law converges to the model posterior,

$$\|\mathcal{L}(G_{1:T}^j, \alpha^j, \lambda^j) - \mathcal{L}(G_{1:T}, \alpha, \lambda \mid G_T, G_1)\|_{\text{TV}} \xrightarrow{j \to \infty} 0.$$
 (19)

4.5. Related work. Existing work on the use of sampling algorithms for inference in sequential network models mainly follows one of two general approaches: Importance sampling [57], or approximate Bayesian computation (ABC) schemes [52].

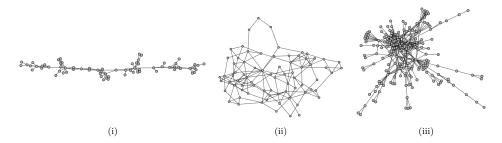


Fig 3. Network data examples: (i) the largest connected component of the NIPS co-authorship network, 2002-03 [26]; (ii) San Juan Sur family ties [40]; (iii) protein-protein interactome [13].

ABC relies on heuristic approximations of the likelihood, and is not guaranteed to sample from the correct target distribution. The basic approach used aboveconduct inference by imputing graph sequences generated by a suitable sampler seems to be due to Wiuf et al. [57], based on earlier work by Griffiths and Tavaré [28] on ancestral inference for coalescent models. More recently, similar approaches have appeared in the "network archeology" literature [43]. See, e.g. Young et al. [59] and references therein. The work of Wang et al. [55], Jasra et al. [34] is related to ours in that they employ particle MCMC, for particular sequential models. Bloem-Reddy et al. [8] exploit the simple probabilistic structure in preferential attachment models to construct a Gibbs sampler that infers the vertex arrival order. All of these methods are, in short, applicable if the sequential model in question is very simple. Otherwise, they suffer (1) from the high variance of estimates that is a hallmark of importance sampling [21], or (2) infeasible computational cost. The algorithm of Wang et al. [55], for example, samples backwards through the sequence generated by the model, and for each reverse step $G_t \to G_{t-1}$ requires computing the probability of every possible forward step $G'_{t-1} \to G_t$ under the given model; even for the (still rather simple) random walk model, that is no longer practical.

Inference techniques developed for models of longitudinal network data are similar in spirit to those developed here, though they typically require observations at each time step. A MCMC algorithm for continuous-time dynamic network models observed at discrete intervals was developed by Koskinen and Snijders [37]; that requires a network of fixed size and are not suitable for growing networks.

5. Experimental evaluation. This section evaluates properties of the model on real-world data and compares its performance to other network models. We also discuss the interpretation of the random walk parameter as a length scale, and of the latent order Π as a measure of centrality.

We consider three network datasets, shown in Figure 3, that exhibit a range of characteristics. The first is the largest connected component (LCC) of the NIPS co-authorship network in 2002-03, extracted from the data used in [26]. As shown in Figure 3, it has a global chain structure connecting highly localized communities. The second dataset represents ties between families in San Juan Sur (SJS), a community in rural Costa Rica [40, 5], and is chosen here as an example of a network with small diameter. The third is the protein-protein interactome (PPI)

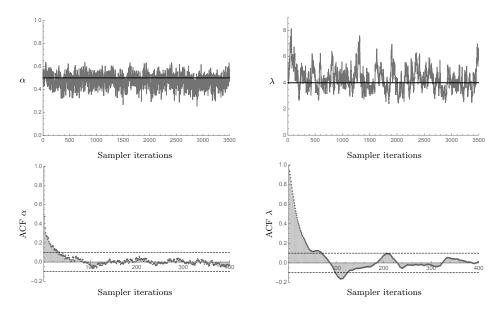


Fig 4. Top: Posterior sample traces for a PG sampler fit to a synthetic graph G_T generated with $\alpha = 0.5$ and $\lambda = 4$ (solid black lines). Bottom: The corresponding autocorrelation functions.

of [13]. The PPI exhibits features such as chains, pendants, and heterogeneously distributed hubs. Basic summary statistics are as follows:

Dataset	Vertices	Edges	Clustering coeff.	Diameter	Mean L_2 -mixing time of $r.w.$
NIPS	70	114	0.70	14	57.3
SJS	75	155	0.32	7	8.4
PPI	230	695	0.32	11	9.1

None of these data sets is particularly large: Sampler diagnostics show graphs of this size suffice to reliably recover model parameters under the random walk model.

Using Algorithm 4, the posterior distributions of α and λ for both the uniform and the size-biased $\mathbf{RW}(\alpha, \mathrm{Poisson}_+(\lambda))$ model can be sampled. Kernel-smoothed posterior distributions under all three datasets are shown in Figure 6. Although posteriors in the uniform and size-biased case are very similar, these models generate graphs with different characteristics for identical parameter values (see Section 5.3).

5.1. Sampler diagnostics (synthetic data). To assess sampler performance, we test the sampler's ability to recover parameter values for graphs generated by the model: A single graph G_T with T=250 edges is generated for fixed values of α and λ . The joint posterior distribution of α and λ given G_T is then estimated using Algorithm 4 (with N=100 particles). Regardless of the input parameter value, a uniform prior is chosen for α , and a Gamma(1,1/4) prior for λ . For the sake of brevity, we report results only for the $\mathbf{RW}_{\mathbf{U}}(\alpha, \operatorname{Poisson}_{+}(\lambda))$ model, on simple graphs (which pose a harder challenge for inference than multigraphs, cf.

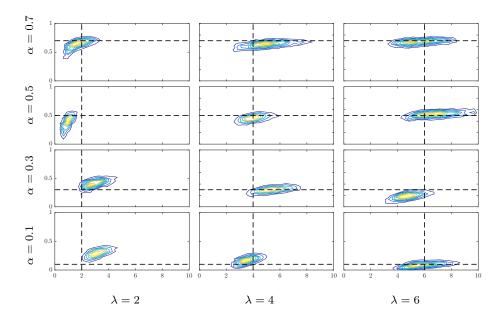


Fig 5. Joint posterior distributions, given graphs generated from an RW_U model. α is on the vertical, λ on the horizontal axis. Generating parameter values are shown by dashed lines.

Section 3.2). Figure 4 shows sampler traces and autocorrelation functions. The samplers mix and converge quickly, and as one would expect, only λ displays any noticeable autocorrelation. Posteriors are shown in Figure 5. Clearly, recovery of model parameters from a single graph is possible. The effect of constraining to simple graphs—the use of step (3') rather than (3) in Algorithm 1—is apparent for $\lambda = 2$: For small values of λ , a significant proportion of random walks ends at their starting point, resulting in the insertion of a new vertex. Since new vertices are otherwise inserted as an effect of α , parameters correlate in the posterior, as visible in Figure 5 for intermediate values of α .

5.2. Length scale. The distance of vertices that can form connections is governed by the parameter λ of the random walk, which can hence be interpreted as a form of length-scale. This scale can be compared to the mean (over starting vertices) mixing time of a random walk on the observed graph, as listed in the table above for each data set: If λ is significantly smaller, the placement of edges inserted by the random walk strongly depends on the graph structure; if λ is large relative to mixing time, dependence between edges is weak.

- In Figure 6, concentration of the λ -posterior on small values in [1,2] for the NIPS data thus indicates predominantly short-range dependence in the data and, since the mixing time is much larger, strong dependence between edges. Concentration of the α -posterior near the origin means connections are mainly formed through existing connections.
- In the SJS network, the posterior peaks near $\lambda = 6$, and hence near the mean

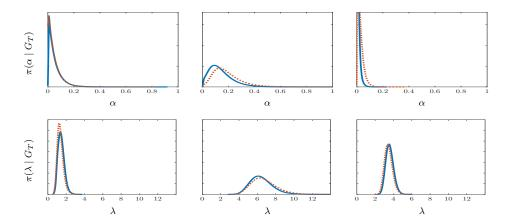


FIG 6. Kernel-smoothed estimates of the model posteriors of RW_U (blue/solid) and $RW_{\rm SB}$ (orange/dotted). Left column: NIPS data. Middle: SJS. Right: PPI. (1000 samples each, at lag 40, after 1000 burn-in iterations; 100 samples each are drawn from 10 chains).

mixing time, with α again small. Thus, the principal mechanism for inserting edges under the model is again the random walk, but a random walk of typical length has almost mixed. Hence, the local connections it creates do not strongly influence each other.

• The PPI network exhibits an intermediate scale of dependence, with most posterior mass in the range $\lambda \in [3, 5]$. Although structures like pendants and chains indicate strong local dependence, there are also denser, more homogeneously connected regions that indicate weaker dependence with longer range.

5.3. Model fitness. Assessing model fitness on network data is difficult: For other types of data, cross validation is often the tool of choice, and indeed, cross-validated link prediction (where links and non-links are deleted uniformly and independently at random) is widely used for evaluation in the machine learning literature. Even if link prediction is considered the relevant statistic of interest, however, cross-validating network data requires subsampling the observed network. Any choice of such a subsampling algorithm implies strong assumptions on how the data was generated; it may also favor one model over another.

We therefore use a protocol developed by Hunter et al. [31], who compare models to data by fixing a set of network statistics. The fitted model is evaluated by comparing the chosen statistics of the data to those of networks simulated from the model. The selected statistics specify which properties are considered important in assessing fit. To capture a range of structures, the following count statistics are proposed in [31], which we also adopt here:

- Normalized degree statistics (ND), d_k , the number of vertices of degree k, divided by the total number of vertices.
- Normalized edgewise shared partner statistics (NESP), χ_k , the number of unordered, connected pairs $\{i,j\}$ with exactly k common neighbors, divided by the total number of edges.

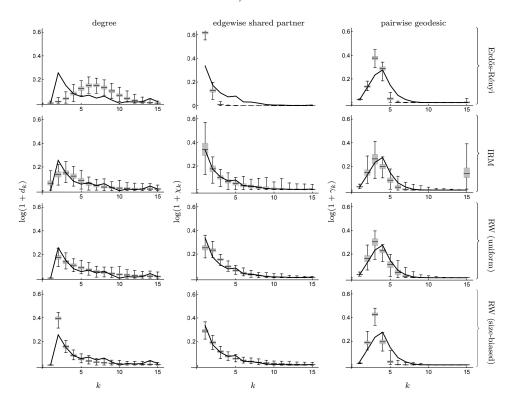


FIG 7. Estimated PPDs for the PPI data set of three statistics: Normalized degree d_k , normalized edgewise shared partner statistic χ_k , and normalized pairwise geodesic γ_k . Results are shown for four models: Erdős-Rényi (top row), IRM (second row), \mathbf{RW}_{U} (third row), and $\mathbf{RW}_{\mathrm{SB}}$ (bottom row). The black line represents the distribution from the PPI data.

• Normalized pairwise geodesic statistics (NPG), γ_k , the number of unordered pairs $\{i, j\}$ with distance k in the graph, divided by the number of dyads.

In a Bayesian setting, executing the protocol amounts to performing posterior predictive checks [11, 25] via the following procedure:

- (1) Sample the model parameters from the posterior, $\theta \sim \pi(\theta|G_T)$.
- (2) Simulate a graph of the same size as the data, $G^{(s)} \sim P(G|\theta)$.
- (3) Calculate the statistic(s) of interest for the simulated graph, $f(G^{(s)})$.

The value $f(G^{(s)})$ is then a sample from the posterior predictive distribution (PPD) of the statistic f under the model. Small PPD mass around the observed value of f indicates the model does not explain those properties of the data that f measures.

PPDs are estimated for the following models: The Erdős-Rényi model (ER); the infinite relational model (IRM) with a Chinese Restaurant Process prior on the number of blocks [35]; the infinite edge partition model with a hierarchical gamma process (EPM) [60]; the ACL model (Section 3.4); and the \mathbf{RW}_{U} and \mathbf{RW}_{SB} models. The table lists total variation distance between the empirical distribution of each statistic on the observed graph and on graphs generated from the respective models.

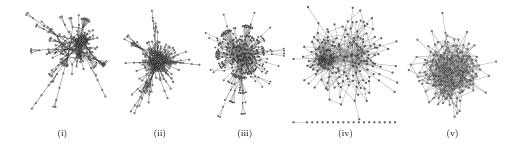


FIG 8. Reconstructions of the PPI network (i), sampled from the posterior mean of (ii) the RW_U model, (iii) the RW_{SB} model, (iv) the IRM, and (v) the Erdős-Rényi model.

Standard errors are computed over 1000 samples. Smaller values indicate a better fit:

		$PPI\ data$			$NIPS\ data$	
Model	Degree	ESP	Geodesic	Degree	ESP	Geodesic
EPM	$0.49 \pm .03$	$0.31 \pm .07$	$0.65 \pm .04$	$0.57 \pm .06$	$0.43 \pm .15$	$0.72 \pm .05$
$_{\rm IRM}$	$0.30 \pm .04$	$0.15 \pm .07$	$0.25 \pm .07$	$0.29 \pm .08$	$0.46 \pm .10$	$0.36 \pm .13$
ER	$0.57 \pm .02$	$0.45 \pm .03$	$0.23 \pm .02$	$0.26 \pm .06$	$0.69 \pm .06$	$0.41 \pm .06$
ACL	$0.28 \pm .02$	$0.09 \pm .02$	$0.34 \pm .03$	$0.42 \pm .05$	$0.51 \pm .06$	$0.50 \pm .04$
RW-U	$0.23 \pm .03$	$0.17 \pm .02$	$0.16\pm.08$	$0.26 \pm .04$	$0.33 \pm .05$	$0.22 \pm .08$
RW-SB	$0.27 \pm .02$	$0.11 \pm .02$	$0.34 \pm .04$	$0.42 \pm .05$	$0.39 \pm .06$	$0.45 \pm .07$

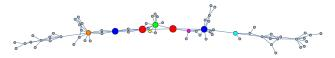
For the ER model, the IRM, and the two random walk models, PPD estimates are shown in more detail in Figure 7, on a logarithmic scale. In terms of the protocol of [31], the uniform random walk model provides the best fit on both data sets. The IRM does similarly well, although it does place significant posterior mass on d_0 and γ_{∞} (since it tends to generate isolated vertices). The good fit comes at the price of model complexity: The IRM is a prior on stochastic blockmodels with an infinite number of classes, a finite number of which are invoked to explain a finite graph. For the PPI data set, for example, the posterior sharply concentrates at 9 classes, which amounts to 53 scalar parameters, compared to 2 for the RW model.

Figure 8 compares reconstructions of a data set from different fitted models. Such visual comparisons should be treated with caution, but the plots underscore that for some types of data, random walk models provide an arguably better structural fit.

5.4. Latent order and vertex centrality. Centrality refers to the importance of a vertex for interactions in a network. A simple measure of centrality is vertex degree; others include Eigenvalue, Katz and Information Centrality [e.g. 44]. Under a **RW** model, the number of random walks passing through a vertex is an obvious measure of its importance to the formation process. A simpler proxy is the vertex insertion order $S_{1:T}$. If only the final graph G_T is observed, the order is given by the posterior of the bridge $G_{1:T}$. The median posterior order under the \mathbf{RW}_{U} model is listed below for the NIPS dataset, for those authors with earliest median appearance, compared to other centrality measures. Listed are ranks of vertices according to each measure, with numerical values in parentheses.

 Sam_I	oling	Order	Degree	Btwn. Cent.	Info. Cent.	Katz Cent.
	(r)	1 (6)	14 (4)	2 (2376)	1 (0.4478)	6 (0.2380)
	(1)	1(6)	4(8)	3(2340)	2(0.4443)	2(0.3740)
	(r)	2(7)	1(12)	1(2797)	3(0.4374)	3(0.2571)
	(1)	2(7)	8 (6)	5 (2116)	5(0.4178)	4(0.2539)
•		3(8)	2(10)	11 (728)	4(0.4259)	1(0.3789)
•		4(10)	2(10)	4(2196)	$11 \ (0.3877)$	5(0.2458)
•		5(12)	14 (4)	6 (1870)	17 (0.3645)	$35 \ (0.0667)$
0		6(13)	14(4)	16 (173)	6(0.4040)	19 (0.1291)

Although one would expect vertices appearing earlier to have larger degree, S seems to correlate more closely with Betweenness Centrality and Information Centrality than with vertex degree. The vertices above correspond to the following vertices in the graph:



- **6. Discussion and open questions.** The models introduced here account for dependence of new links on existing links, but are nonetheless tractable. In light of our results, there are two reasons for tractability:
 - The effects of the parameters α and λ are sufficiently distinct that inference is possible—a single graph generated by the model carries sufficient signal for parameter values to be recovered with high accuracy, as evident in Figure 5.
 - There exists a latent variable—the edge insertion order Π —conditioning on which greatly simplifies the distribution of $(\alpha, \lambda) \mid G_T$.

Conditioning on history information is instrumental both for theoretical results and for inference. As noted in the introduction, a qualitatively similar effect—the joint distribution of the network graph simplifies conditionally on a suitable latent variable—is observed in other popular random graph models.

The inference algorithms in Section 4 work well for moderately sized graphs (of up to a few hundred vertices). The dominant source of computational complexity is sampling the edge order—similar to inference algorithms for graphon models (which have comparable input size limitations), although the latent order plays a very different role here than in an exchangeable model. Although improvements in efficiency or approximations are certainly possible, we do not expect the methods to scale to very large graphs. Such graphs are not the subject of this work. It is crucial that, under the random walk model, graphs of feasible size do provide sufficient data for reliable inference. For more complicated models, that might not be the case.

To conclude, we note there are open questions beyond the scope of this paper. Some of these are obvious, such as applications to dynamic network problems; generalizations to disconnected graphs (e.g. using a disconnected seed graph); or which choices of the distribution P of the random walk length in Theorem 3.3

satisfy condition (6). We also mention two open questions that seem intriguing, but non-trivial:

- 1) The generative process (Algorithm 1) starts with an initial "seed graph" G_1 . In our experiments, G_1 simply consists of a single edge, but one might choose any finite graph instead. For example, if a graph g of a given, finite size is observed, and interpreted as the outcome of a random walk model after t steps, one could perform predictive analysis by considering the random graph $G_T|G_1=g$, now with t+T-1 edges. For preferential attachment models, it has been shown that the choice of such a seed graph G_1 can have significant influence on the resulting graph G_T that remains detectable even in the limit $T\to\infty$ [12]. The structure of our model seems to suggest a similar property: The results Section 3.3 show, roughly speaking, that properties similar to those of preferential attachment models hold for the limiting degree sequence if one conditions on the vertex arrival time sequence S. It is not clear, however, whether and how the techniques used by Bubeck $et\ al$. [12] are applicable to the random walk model.
- 2) Another open question is whether the random walk itself results in power law behavior: The results in Section 3 stem from size-biased sampling, not the random walk. The \mathbf{RW}_{U} model on multigraphs, however, does not use such reinforcement, but empirically exhibits heavy-tailed degrees nonetheless. Intuitively, the probability to reach a vertex by random walk increases with degree: For any $\mathbf{RW}(\alpha, P)$ model, the probability (1) can be written as

$$\mathbb{P}\{V_{end} = v | V_0 = u, G\} = \left[\frac{d_v}{\text{vol}(G)} + \sqrt{\frac{d_v}{d_u}} \sum_{i=2}^n H_P(1 - \sigma_i) \psi_i(u) \psi_i'(v)\right],$$

where (ψ_i) are the eigenvectors, and (σ_i) the eigenvalues, of the Laplacian L. Thus, the probability to terminate at v is a mixture of a preferential attachment term (proportional to d_v), and a term depending on P and on the structure of G at various scales. That seems to suggest the random walk induces a power law, but at present, we have no proof.

APPENDIX A: PROOFS

A.1. Proof of Proposition 3.1. If K has law Poisson₊(λ), (1) becomes

$$Q^{\lambda} = \sum_{k=0}^{\infty} \frac{e^{-\lambda} \lambda^{k}}{k!} (D^{-1}A)^{k+1} = D^{-1/2} \left[(\mathbb{I}_{n} - \mathbf{L}) e^{-\lambda} \sum_{k=0}^{\infty} \frac{\lambda^{k} (\mathbb{I}_{n} - \mathbf{L})^{k}}{k!} \right] D^{1/2}$$
$$= D^{-1/2} \left[(\mathbb{I}_{n} - \mathbf{L}) e^{-\lambda \mathbf{L}} \right] D^{1/2} = D^{-1/2} \left[(\mathbb{I}_{n} - \mathbf{L}) \mathbf{K}^{\lambda} \right] D^{1/2}.$$

Since the spectral norm of $\mathbb{I}-\mathbf{L}$ is 1, series is absolutely convergent. For $K \sim \mathrm{NB}_+(r,p)$,

$$\sum_{k=0}^{\infty} \frac{\Gamma(k+r)}{\Gamma(k+1)\Gamma(r)} p^k (1-p)^r (D^{-1}A)^{k+1} = D^{-1/2} \left[(\mathbb{I}_n - \mathbf{L}) \left(\mathbb{I}_n + \frac{p}{1-p} \mathbf{L} \right)^{-r} \right] D^{1/2}$$
(20)

similarly yields $Q^{r,p} = D^{-1/2} [(\mathbb{I}_n - \mathbf{L}) \mathbf{K}^{r,p}] D^{1/2}$.

A.2. Proof of Theorem 3.3. We begin with a lemma used in the proofs of Theorem 3.3 and Theorem 3.4. Let $\delta_j^{(1)}(t)$ be an indicator variable that is equal to 1 if the first end of the t-th edge is attached to vertex v_j , and 0 otherwise; likewise define $\delta_i^{(2)}(t)$ for the second end of the t-th edge.

LEMMA 1. Suppose a sequence of graphs is generated with law $\mathbf{RW}_{\text{SB}}(\alpha, P)$, such that P is a probability distribution on \mathbb{N} . Then the size-biased distribution \mathbb{S}_t is left-invariant under the mixed random walk probability Q_t induced by P, that is

$$\mathbb{S}'_t Q_t = \mathbb{S}'_t \qquad \text{where } [Q_t]_{uv} := \mathbb{P}\{V_{end} = v \,|\, V_0 = u, G_t\}$$
 (21)

holds for every $t \in \mathbb{N}_+$. Furthermore, for each $v_i \in \mathcal{V}(G_t)$, the following holds:

$$\mathbb{E}[\delta_j^{(1)}(t+1) \mid G_t] = \frac{1}{1-\alpha} \mathbb{E}[\delta_j^{(2)}(t+1) \mid G_t] = \frac{\deg_t(v_j)}{2t} . \tag{22}$$

PROOF. Substituting (1) into $\mathbb{S}'_t Q_t$ yields

$$\mathbb{S}'_t Q_t = \sum_k \mathbb{S}'_t (D^{-1} A)^k P\{K = k\} = \sum_k \mathbb{S}'_t P\{K = k\} = \mathbb{S}'_t . \tag{23}$$

The $\mathbf{RW}_{\mathtt{SB}}$ model samples the first end of each edge from the size-biased distribution:

$$\mathbb{E}[\delta_j^{(1)}(t+1) \mid G_t] = \mathbb{P}[V_{t+1} = v_j \mid G_t] = \frac{\deg_t(v_j)}{2t} . \tag{24}$$

For the second end, denote by $\mathbb{1}_{j,t}$ the indicator vector for vertex v_j . Then

$$\mathbb{E}[\delta_j^{(2)}(t+1) \mid G_t] = \sum_{u} \mathbb{P}[V_{t+1} = u \mid G_t] [Q_t]_{uv} = (1-\alpha) \mathbb{S}'_t Q_t \mathbb{1}_{j,t} = (1-\alpha) \frac{\deg_t(v_j)}{2t} .$$

In the setup of Theorem 3.3, asymptotic expected degree counts are as follows:

LEMMA 2. Let a sequence of multigraphs $(G_1, G_2, ...)$ have law $\mathbf{RW}_{\text{SB}}(\alpha, P)$, for a probability distribution P on \mathbb{N} satisfying Equation (6). Then

$$\frac{\mathbb{E}[m_{d,t}]}{\alpha t} \xrightarrow{a.s.} p_d \qquad \text{for each } d \in \mathbb{N} \text{ as } t \to \infty , \qquad (25)$$

where p_d is given in (5).

PROOF. Equation (6) yields the recurrence

$$\mathbb{E}(m_{d,t+1}) = \alpha \cdot \delta_1(d) + \mathbb{E}(m_{d,t}) \left(1 - \frac{(2-\alpha)d}{2t}\right) + \mathbb{E}(m_{d-1,t}) \frac{(2-\alpha)(d-1)}{2t} + o(1) ,$$

with $m_{0,t} = 0$ for all t. This can be written more generally as

$$M(d, t+1) = (1 - b(t)/t)M(d, t) + g(t).$$
(26)

If $b(t) \to b$ and $g(t) \to g$, then $M(d,t)/t \to g/(b+1)$, by [22, Lemmas 4.1.1, 4.1.2]. For d=1, we have $b(t)=b=(2-\alpha)/2$ and $g(t)=g=\alpha$, so $\mathbb{E}(m_{1,t})/t \to \frac{2\alpha}{4-\alpha}=\alpha p_1$. Proceeding by induction, $b=(2-\alpha)d/2$ and $g=\alpha p_{d-1}(2-\alpha)(d-1)/2$ yield

$$\frac{\mathbb{E}[m_{d,t}]}{\alpha t} \to p_{d-1} \frac{(2-\alpha)(d-1)}{2+(2-\alpha)d} = \frac{2}{4-\alpha} \prod_{j=1}^{d-1} \frac{j}{\frac{2}{2-\alpha}+j+1} = \frac{2}{2-\alpha} \frac{\Gamma(d)\Gamma(2+\frac{\alpha}{2-\alpha})}{\Gamma(d+2+\frac{\alpha}{2-\alpha})} ,$$

for
$$d > 1$$
, which is just p_d as defined in (5).

The following result, the proof of which can be found in Chung and Lu [17, Sec. 3.6] shows that the random variable $m_{d,t}$ concentrates about its mean:

LEMMA 3. Let a sequence of multigraphs $(G_1, G_2, ...)$ have law $\mathbf{RW}_{\text{SB}}(\alpha, P)$, for a probability distribution P on \mathbb{N} satisfying Equation (6). Then

$$\mathbb{P}\left[\left|\frac{m_{d,t}}{\alpha t} - p_d\right| \le 2\sqrt{\frac{d^3 \log t}{\alpha^2 t}}\right] \ge 1 - 2(t+1)^{d-1}t^{-d} = 1 - o(1). \tag{27}$$

PROOF OF THEOREM 3.3. Lemma 3 shows that $\frac{m_{d,t}}{\alpha t}$ concentrates around its mean, and with Lemma 2 showing that the mean is p_d , the proof of the theorem is complete.

A.3. Proof of Theorem 3.4. By definition of **RW** models (see Algorithm 1), at each step t a new vertex appears with probability α , which is represented as a collection of Bernoulli(α) random variables $(B_t)_{t\geq 2}$. Alternatively, there is the collection of steps $S_1, S_2, \ldots, S_j, \ldots$ at which new vertices appear, such that S_j is the step at which the j-th vertex appears. By the fundamental relationship between

Bernoulli and Geometric random variables, the sequence $S_1, S_2, \ldots, S_j, \ldots$ can be sampled independently of the graph sequence as $S_1 = S_2 = 1$ and

$$S_j = S_{j-1} + \Delta_j$$
, where $\Delta_j \stackrel{\text{iid}}{\sim} \text{Geometric}(\alpha)$, for $j > 2$. (28)

In what follows, we condition on the sequence $(S_j)_{j\geq 1}$ unless explicitly stated otherwise. We begin by calculating the expected degree of the *j*-th vertex.

LEMMA 4. Let a sequence of multigraphs $(G_1, G_2, ...)$ have law $\mathbf{RW}_{SB}(\alpha, P)$. Let $d_j(t) := \deg_t(v_j)$ be the degree of v_j in graph G_t , where v_j is the j-th vertex to appear in the graph sequence, and let $\rho = 1 + \frac{\alpha}{2-\alpha}$. Then conditional on S_j , $d_j(t)t^{-1/\rho}$ converges almost surely to a random variable ξ_j as $t \to \infty$, and

$$\mathbb{E}[d_j(t) \mid S_j] = \frac{\Gamma(S_j)\Gamma(t + \frac{1}{\rho})}{\Gamma(S_j + \frac{1}{\rho})\Gamma(t)}$$
(29)

PROOF. Let A_t denote the σ -algebra generated after t steps. Then for $t \geq S_j$,

$$\mathbb{E}[d_j(t+1) \mid \mathcal{A}_t] = d_j(t) + \mathbb{E}[\delta_j^{(1)}(t+1) \mid \mathcal{A}_t] + \mathbb{E}[\delta_j^{(2)}(t+1) \mid \mathcal{A}_t] = d_j(t)(1 + \frac{1}{at}), \quad (30)$$

where the final identity follows from Lemma 1, and $d_i(S_i) = 1$. The sequence

$$M_j(t) := d_j(t) \frac{\Gamma(S_j + \frac{1}{\rho})}{\Gamma(S_j)} \cdot \frac{\Gamma(t)}{\Gamma(t + \frac{1}{\rho})} \quad \text{for } t \ge S_j$$
 (31)

is a non-negative martingale with mean 1, by (30). Therefore, $M_j(t)$ converges almost surely to a random variable M_j as $t \to \infty$. Taking expectations on both sides and rearranging (31) yields (29). With Stirling's formula,

$$\frac{d_j(t)}{t^{1/\rho}} \xrightarrow{\text{a.s.}} M_j \frac{\Gamma(S_j)}{\Gamma(S_j + \frac{1}{\rho})} := \xi_j . \tag{32}$$

We now consider the joint distribution of the limiting random variables $(\xi_j)_{j\geq 1}$. The approach, which is adapted from [42] (see also [22]), is to analyze a martingale that yields the moments of $(\xi_j)_{j\geq 1}$. First, define for $t\geq S_j$,

$$R_{j,k}(t) := \frac{\Gamma(d_j(t) + k)}{\Gamma(d_j(t))\Gamma(k+1)} , \qquad (33)$$

At a high level, $R_{j,k}(t) \approx d_j(t)^k/k!$ for large t, so (32) shows that properly scaled $R_{j,k}(t)$ should converge to $\xi_j^k/k!$ for each j. We make this precise in what follows.

Let $\vec{j} := (j_i)$ be an ordered collection of vertices such that $1 \le j_1 < j_2 < \cdots < j_r$, and let $\vec{k} := (k_i)$ be a corresponding vector of moments. To define a suitable martingale, we abbreviate

$$\mu_{\vec{k}} := \sum_{i=1}^r k_i \quad \text{ and } \quad \Sigma_{\vec{j}, \vec{k}}(t) := \sum_{i,l=1}^r \left(\frac{1}{2}\right)^{\mathbb{1}_{i=l}} \frac{k_i(k_l - \mathbb{1}_{i=l})}{d_{j_l}(t) + \mathbb{1}_{i=l}} [Q_t]_{j_i j_l} ,$$

and note $[Q_t]_{jj'} = 0$ for all $t < \max\{S_j, S_{j'}\}$. Define

$$c_{\vec{j},\vec{k}}(t) = \Gamma(t) \left[\prod_{s=0}^{t-1} \left(s + \frac{\mu_{\vec{k}}}{\rho} + \frac{1-\alpha}{2} \Sigma_{\vec{j},\vec{k}}(s) \right) \right]^{-1}, \tag{34}$$

which is a random variable since Q_t is random, and is \mathcal{A}_t -measurable for each t. Since $[Q_t]_{j_ij_i} < 1$, and since $d_j(t) \xrightarrow{\text{a.s.}} \infty$ as $t \to \infty$ by Lemma 4, $\Sigma_{\vec{j},\vec{k}}(t) \xrightarrow{\text{a.s.}} 0$ as $t \to \infty$, which yields

$$c_{\vec{j},\vec{k}}(t) = \frac{\Gamma(t)}{\Gamma(t + \frac{1}{o}\mu_{\vec{k}})} (1 + o(1)) = t^{-\mu_{\vec{k}}/\rho} (1 + o(1)) \quad \text{as } t \to \infty . \tag{35}$$

Note that

$$\lim_{t \to \infty} c_{\vec{j}, \vec{k}}(t) \prod_{i=1}^{r} R_{j_i, k_i} = \prod_{i=1}^{r} \frac{\xi_{j_i}^{k_i}}{\Gamma(k_i + 1)} , \qquad (36)$$

if the limit exists. Existence is based on the following result:

LEMMA 5. Let A_t denote the σ -algebra generated by a $\mathbf{RW}_{SB}(\alpha, P)$ multigraph sequence up to step t. Let r > 0 and $1 \le j_1 < j_2 < \cdots < j_r$ be integers, and real-valued $k_1, k_2, \ldots, k_r > -1$. Then with $R_{j,k}(t)$ defined in (33) and $c_{\vec{j},\vec{k}}(t)$ defined in (34),

$$Z_{\vec{j},\vec{k}}(t) := c_{\vec{j},\vec{k}}(t) \prod_{i=1}^{r} R_{j_i,k_i}(t)$$
(37)

is a nonnegative martingale for $t \ge \max\{S_{j_r}, 1\}$. If $k_1, k_2, \ldots, k_r > -\frac{1}{2}$, then $Z_{\vec{j}, \vec{k}}(t)$ converges in L_2 .

PROOF. It can be shown that

$$\mathbb{E}\Big[\prod_{i=1}^{r} R_{j_{i},k_{i}}(t+1) \mid \mathcal{A}_{t}\Big] = \Big(\prod_{i=1}^{r} R_{j_{i},k_{i}}(t)\Big) \Big(1 + \frac{\mu_{\vec{k}}}{\rho t} + \frac{1-\alpha}{2t} \Sigma_{\vec{j},\vec{k}}(t)\Big) , \qquad (38)$$

from which it follows that

$$\mathbb{E}[Z_{\vec{j},\vec{k}}(t+1) \mid \mathcal{A}_t] = c_{\vec{j},\vec{k}}(t+1)R_{\vec{j},\vec{k}}(t)\left(1 + \frac{\mu_{\vec{k}}}{\rho t} + \frac{1-\alpha}{2t}\Sigma_{\vec{j},\vec{k}}(t)\right) = c_{\vec{j},\vec{k}}(t)R_{\vec{j},\vec{k}}(t) = Z_{\vec{j},\vec{k}}(t) . \tag{39}$$

Furthermore, $Z_{\vec{i},\vec{k}}(\max\{S_{j_r},1\}) > 0$. By (35) and properties of the gamma function,

$$Z_{\vec{j},\vec{k}}(t)^2 \le Z_{\vec{j},2\vec{k}}(t) \prod_{i=1}^r \binom{2k_i}{k_i} .$$
 (40)

By (39), $Z_{\vec{j},2\vec{k}}(t)$ is a martingale with finite expectation for $2k_1,\ldots,2k_r>-1$. Therefore, $Z_{\vec{j},\vec{k}}(t)$ is an L_2 -bounded martingale and hence converges in L_2 (and also in L_1) for $k_1,\ldots,k_r>-\frac{1}{2}$.

Combining the auxiliary results above, we can now give proof of the result.

PROOF OF THEOREM 3.4. The limit of $Z_{\vec{j},\vec{k}}(t)$ is (36), which enables calculation of the moments of ξ_j . In particular, for any vertex v_j , $j \in \mathbb{N}_+$, $k \in \mathbb{R}$ such that $k > -\frac{1}{2}$,

$$\mathbb{E}\left[\frac{\xi_j^k}{\Gamma(k+1)} \mid S_j\right] = \lim_{t \to \infty} \mathbb{E}[Z_{j,k}(t) \mid S_j] = \mathbb{E}[Z_{j,k}(S_j) \mid S_j] = \frac{\Gamma(S_j)}{\Gamma(S_j + \frac{k}{a})}. \tag{41}$$

Although the joint moments involve $\Sigma_{\vec{j},\vec{k}}$, the moments (41) characterize the marginal distribution of $\xi_i \mid S_i$ via the Laplace transform. Since

$$\mathbb{E}[\xi_j^k \mid S_j] = \frac{\Gamma(S_j)\Gamma(k+1)}{\Gamma(S_j + \frac{k}{\varrho})} = \frac{\Gamma\left(\rho(S_j - 1) + 1 + k\right)\Gamma(S_j)}{\Gamma\left(\rho(S_j - 1) + 1\right)\Gamma\left(S_j + \frac{k}{\varrho}\right)} \frac{\Gamma\left(\rho(S_j - 1) + 1\right)\Gamma(k+1)}{\Gamma\left(\rho(S_j - 1) + 1 + k\right)},$$

 $\mathbb{E}[\xi_j^k \mid S_j] = \mathbb{E}[M_j^k B_j^k \mid S_j]$, where M_j is a generalized Mittag-Leffler $(\rho^{-1}, S_j - 1)$ variable [32], and B_j is $B_j \sim \text{Beta}(1, \rho(S_j - 1))$. It follows that $M_j \perp \!\!\!\perp_{S_j} B_j$. The second equality in distribution is verified by checking moments.

It remains to show (9). We begin by noting that the left-hand side of (41) is an expectation that conditions on S_j . Define $\tilde{S}_j := S_j - 1 - (j-2)$, which is marginally distributed as $NB(j-2, 1-\alpha)$. Then

$$\mathbb{E}\left[\mathbb{E}[\xi_{j}^{k} \mid S_{j}]\right] = \mathbb{E}\left[\frac{\Gamma(\tilde{S}_{j}+1+(j-2))\Gamma(k+1)}{\Gamma(\tilde{S}_{j}+1+(j-2)+\frac{k}{\rho})}\right]
= \sum_{t=0}^{\infty} \frac{\Gamma(t+1+(j-2))\Gamma(k+1)}{\Gamma(t+1+(j-2)+\frac{k}{\rho})} \frac{\Gamma(t+j-2)}{\Gamma(j-2)\Gamma(t+1)} (1-\alpha)^{t} \alpha^{j-2}$$

$$= \frac{\Gamma(k+1)\Gamma(j-1)}{\Gamma(j-1+\frac{k}{\rho})} \alpha^{\frac{k}{\rho}} {}_{2}F_{1}(1+\frac{k}{\rho},\frac{k}{\rho};j-1+\frac{k}{\rho};1-\alpha) ,$$
(42)

where ${}_{2}F_{1}(a,b;c;z)$ is the ordinary hypergeometric function. For $j \to \infty$,

$$\lim_{j \to \infty} \mathbb{E} \big[\mathbb{E} [\xi_j^k \mid S_j] \big] = \lim_{j \to \infty} \frac{\Gamma(k+1)\Gamma(j-1)}{\Gamma(j-1+\frac{k}{\rho})} \alpha^{\frac{k}{\rho}} (1 + O(j^{-1})) = \Gamma(k+1) \alpha^{\frac{k}{\rho}} j^{-\frac{k}{\rho}} (1 + O(j^{-1})) .$$

follows using the series expansion of ${}_{2}F_{1}(a,b;c;z)$.

A.4. Proof of Proposition 3.5.

PROOF OF PROPOSITION 3.5. Existence of the limit as $\lambda \to \infty$ follows from the existence of the limiting (stationary) distribution for each $t \in \mathbb{N}_+$. For equivalence, it suffices to show that given any connected graph G, the conditional distribution over graphs G' is the same for $\mathbf{RW}_{\text{SB}}(\alpha,\infty)$ and $\mathbf{ACL}(\alpha)$. The probability of attaching a new vertex to an existing vertex v in both models is $\alpha \deg(v)/\operatorname{vol}(G)$. With probability $1-\alpha$, a new edge is inserted between existing vertices u and v, and so it remains to show that in this case the distribution over pairs of vertices, $\nu(u,v)$, is the same. We have

$$\nu(u,v) = 2 \frac{\deg(u)}{\operatorname{vol}(G)} \frac{\deg(v)}{\operatorname{vol}(G)} \quad \text{ and } \quad \nu(u,v) = \frac{\deg(u)}{\operatorname{vol}(G)} [Q^{\lambda}]_{uv} + \frac{\deg(v)}{\operatorname{vol}(G)} [Q^{\lambda}]_{vu}$$

for the ACL and $\mathbf{RW}_{\mathrm{SB}}$ model respectively, with Q^{λ} . First, consider $(\mathbb{I}_n - \mathbf{L})\mathbf{K}^{\lambda}$ in terms of the spectrum of \mathbf{L} . Let $0 = \sigma_1 \leq \cdots \leq \sigma_n \leq 2$ be the eigenvalues for a graph on n vertices, with eigenvectors ψ_i . Then

$$(\mathbb{I}_n - \mathbf{L})\mathbf{K}^{\lambda} = (\mathbb{I}_n - \mathbf{L})e^{-\lambda \mathbf{L}} = \sum_{i=1}^n (1 - \sigma_i)e^{-\lambda \sigma_i} \psi_i \psi_i'.$$
 (43)

When $\lambda \to \infty$, only the eigenvector ψ_1 corresponding to the eigenvalue $\sigma_1 = 0$ contributes to the random walk probabilities, i.e. $\lim_{\lambda \to \infty} (\mathbb{I}_n - \mathbf{L}) e^{-\lambda \mathbf{L}} = \psi_1 \psi_1'$. The limit satisfies $\psi_1 \propto D^{1/2} \mathbb{1}$, where $\mathbb{1}$ is the vector of all ones [16, Ch. 2]. Therefore,

$$\lim_{\lambda \to \infty} [Q^{\lambda}]_{uv} = \left[\mathbb{1} \mathbb{1}' D_{\overline{\operatorname{vol}(G)}} \right]_{uv} = \frac{\deg(v)}{\operatorname{vol}(G)} ,$$

and the result follows.

A.5. Proofs for Section 4.

PROOF OF PROPOSITION 4.1. Proposition 2.2 of Del Moral and Murray [20] shows that

$$\mathbb{E}[f(G_{1:T}) \mid G_1, G_T] = L_{\theta}^1(G_1)^{-1} \mathbb{E}\left[f(G_{1:T}) L_{\theta}^{T-1}(G_{T-1}) \frac{h_t(G_t)}{h_t(G_{T-1})} \prod_{s=2}^{T-1} \frac{h_s(G_s)}{h_{s-1}(G_{s-1})} \mid G_1\right],$$

for any approximation function h_t that is positive outside a null set. For our choice of h_t , the proposal density (14) only places probability mass on graphs with nonzero bridge likelihood, making $\mathbb{1}\{h_t=0\}$ a probability zero event. For an SMC approximation to be consistent, the target density must be absolutely continuous with respect to the proposal density at each step t [see, e.g. 50, 21]. In other words, the proposal density must be a valid importance sampling distribution at each step. The target, $\mathcal{L}_{\theta}(G_{1:t} \mid G_T, G_1)$ is absolutely continuous with respect to $\prod_{s=2}^t r_{\theta}(G_s \mid G_{s-1})$ from (14) by construction if properties (P1) and (P2) hold, and the result follows.

Proposition 4.2 is a special case of the following:

PROPOSITION A.1. Let q_{θ}^t , for $t=1,\ldots,T$, be the Markov kernels defining a sequential network model that satisfies conditions (P1) and (P2), and let r_{θ}^t be the corresponding proposal kernels. Furthermore, let $h_t(G_T \mid G_t)$ for $t=1,\ldots,T-2$ be a sequence of fixed functions that are strictly positive if $G_t \subseteq G_T$. Given an observation G_T and a fixed G_1 , define the weights

$$\tilde{w}_{t}^{i} := \begin{cases}
1, & for \quad t = 1 \\
\frac{1}{h_{t}(G_{T} \mid G_{t-1}^{i})} \frac{q_{\theta}^{t}(G_{t}^{i} \mid G_{t-1}^{i})}{r_{\theta}^{t}(G_{t}^{i} \mid G_{t-1}^{i})}, & for \quad 2 \leq t < T - 1 \\
\frac{q_{\theta}^{t}(G_{T} \mid G_{t})}{h_{t}(G_{T} \mid G_{t-1}^{i})} \frac{q_{\theta}^{t}(G_{t}^{i} \mid G_{t-1}^{i})}{r_{\theta}^{t}(G_{t}^{i} \mid G_{t-1}^{i})}, & for \quad t = T - 1
\end{cases} , (44)$$

and w_t^i the corresponding weights normalized across the N particles. Define the estimator

$$\hat{L}_{\theta}^{1} := \prod_{t=2}^{T-1} \left[\left(\sum_{i=1}^{N} \frac{\tilde{w}_{t}^{i}}{N} \right) \left(\frac{\sum_{i=1}^{N} h_{t-1} (G_{T} \mid G_{t-1}^{i}) \tilde{w}_{t-1}^{i}}{\sum_{i=1}^{N} \tilde{w}_{t-1}^{i}} \right) \right]$$

$$:= \prod_{t=2}^{T-1} \hat{L}_{\theta} (G_{t} \mid G_{t-1}) .$$

$$(45)$$

Then \hat{L}^1_{θ} is positive and unbiased: $\hat{L}^1_{\theta} > 0$ and $\mathbb{E}[\hat{L}^1_{\theta}] = L^1_{\theta}(G_1) = p_{\theta}(G_T \mid G_1)$, for any $N \geq 1$.

PROOF. Unbiasedness will be established by iterating expectations, following the approach in Pitt *et al.* [48]. Let S_t be the set of particles and weights $\{G_t^i; \tilde{w}_t^i\}$ at step t. Then we have that

$$\begin{split} & \mathbb{E}\left[\left(\sum_{i=1}^{N} \frac{\tilde{w}_{T-1}^{i}}{N}\right) \middle| \mathcal{S}_{T-2}\right] \\ & = \sum_{i=1}^{N} \int \frac{q_{\theta}^{t}(G_{T} \mid G_{T-1})}{h_{T-2}(G_{T} \mid G_{T-2}^{i})} \frac{q_{\theta}^{t}(G_{T-1} \mid G_{T-2}^{i})}{r_{\theta}^{t}(G_{T-1} \mid G_{T-2}^{i})} \frac{r_{\theta}^{t}(G_{T-1} \mid G_{T-2}^{i})h_{T-2}(G_{T} \mid G_{T-2}^{i})\tilde{w}_{T-2}^{i}}{\sum_{j=1}^{N} h_{T-2}(G_{T} \mid G_{T-2}^{i})\tilde{w}_{T-2}^{j}} dG_{T-1} \\ & = \sum_{i=1}^{N} \frac{p_{\theta}^{T,T-2}(G_{T} \mid G_{T-2}^{i})\tilde{w}_{T-2}^{i}}{\sum_{j=1}^{N} h_{T-2}(G_{T} \mid G_{T-2}^{j})\tilde{w}_{T-2}^{j}} . \end{split}$$

Therefore, $\mathbb{E}[\hat{L}_{\theta}(G_{T-1}\mid G_{T-2})\mid \mathcal{S}_{T-2}] = \sum_{i=1}^{N} p_{\theta}^{T,T-2}(G_T\mid G_{T-2}^i)w_{T-2}^i$. Likewise, it is straightforward to show that

$$\mathbb{E}[\hat{L}_{\theta}(G_{T-1} \mid G_{T-2})\hat{L}_{\theta}(G_{T-2} \mid G_{T-3}) \mid \mathcal{S}_{T-3}]$$

$$= \mathbb{E}[\mathbb{E}[\hat{L}_{\theta}(G_{T-1} \mid G_{T-2}) \mid \mathcal{S}_{T-2}] \hat{L}_{\theta}(G_{T-2} \mid G_{T-3}) \mid \mathcal{S}_{T-3}] = \sum_{i=1}^{N} p_{\theta}^{T,T-3}(G_{T} \mid G_{T-3}^{i}) w_{T-3}^{i}.$$

Iterating for $t = T - 4, \dots, 1$, we have

$$\mathbb{E}\left[\prod_{t=2}^{T-1} \left\{ \left(\sum_{i=1}^{N} \frac{\tilde{w}_{t}^{i}}{N}\right) \left(\frac{\sum_{i=1}^{N} h_{t-1}(G_{T} \mid G_{t-1}^{i}) \tilde{w}_{t-1}^{i}}{\sum_{i=1}^{N} \tilde{w}_{t-1}^{i}}\right) \right\} \mid \mathcal{S}_{1}\right]$$

$$= \sum_{i=1}^{N} p_{\theta}^{T,1}(G_{T} \mid G_{1}^{i}) w_{1}^{i} = p_{\theta}(G_{T} \mid G_{1}),$$

which proves the claim.

PROOF OF PROPOSITION 4.3. Theorem 4 of Andrieu *et al.* [3], of which Proposition 4.3 is a special case, requires that: (a) The resampling scheme in the SMC algorithm is unbiased, i.e. each particle is resampled with probability proportional to its

weight. (b) $\mathcal{L}_{\theta}(G_{1:t} \mid G_T, G_1)$ is absolutely continuous with respect to $\prod_{s=2}^t r_{\theta}(G_s \mid G_{s-1})$ for any θ . Condition (a) is satisfied by the multinomial, residual, and stratified resampling schemes. As discussed in the proof of Proposition 4.1, the condition (b) holds by construction if properties (P1) and (P2) hold.

APPENDIX B: PARTICLE GIBBS UPDATES

The particle Gibbs sampler updates are performed in three blocks: (α, λ) , (\mathbf{B}, \mathbf{K}) , and $G_{2:(T-1)}$. As we describe in the following subsections, we make use of conditional conjugacy and tools from spectral graph theory to increase sampling efficiency. We discuss each block of updates in turn.

Updating the parameters α and λ . The model is specified in terms of distributions for the latent variables, and placing conjugate priors on their parameters we have,

$$B_t \mid \alpha \stackrel{\text{iid}}{\sim} \text{Bernoulli}(\alpha), \quad \alpha \sim \text{Beta}(a_{\alpha}, b_{\alpha})$$
 (46)

$$K_t \mid \lambda \stackrel{\text{iid}}{\sim} \text{Poisson}_+(\lambda), \quad \lambda \sim \text{Gamma}(a_\lambda, b_\lambda).$$
 (47)

The Gibbs updates are hence $\alpha \mid \mathbf{B} \sim \text{Beta}(\chi, \omega)$ and $\lambda \mid \mathbf{K} \sim \text{Gamma}(\kappa, \tau)$, with

$$\chi := a_{\alpha} + \sum_{t=2}^{T} B_t, \quad \omega := b_{\alpha} + (T - 1) - \sum_{t=2}^{T} B_t$$
(48)

$$\kappa := a_{\lambda} + \sum_{t=2}^{T} K_t, \quad \tau := b_{\lambda} + (T - 1).$$
(49)

Updating the latent variables **B** and **K**. The sequential nature of the model allows each of the latent variables B_t and K_t to be updated individually. We use conditional independence to marginalize out sampling steps where possible, since such marginalization increase the sampling efficiency. For both **B** and **K**, we marginalize twice: The first transforms the conditional distributions $P(B_t | \alpha)$ and $P(K_t | \lambda)$ into the predictive distributions $P(B_t | \mathbf{B}_{-t})$, and $P(K_t | \mathbf{K}_{-t})$, which yields

$$B_t \mid \mathbf{B}_{-t} \sim \mathrm{Bernoulli}\Big(\frac{\chi_{-t}}{\chi_{-t} + \omega_{-t}}\Big) \quad \text{ and } \quad K_t \mid \mathbf{K}_{-t} \sim \mathrm{NB}_+\Big(\kappa_{-t}, \frac{1}{1 + \tau_{-t}}\Big) \;.$$

The second improvement is made by marginalizing the conditional dependence of B_t on K_t , and of K_t on B_t . That requires some notation: $\delta_t(V_t, U_t)$ indicates that a new edge is added to the graph between vertices V_t and U_t . When a new vertex is attached to V_t , we write $\delta_t(V_t, u^*)$. We abbreviate $\bar{\tau} := \frac{1}{1+\tau}$, and write $\tilde{\mathcal{N}}(v)$ for the $\{0,1\}$ -ball of vertex v, i.e. v and its neighbors. The updates for \mathbf{B} are

$$P(B_{t} = 1 \mid G_{(t-1):t}, \mathbf{K}_{-t}, \mathbf{B}_{-t}) \propto \frac{\delta_{t}(V_{t}, u^{*})\mu_{t-1}(V_{t})\chi_{-t}}{\chi_{-t} + \omega_{-t}}$$

$$P(B_{t} = 0 \mid G_{(t-1):t}, \mathbf{K}_{-t}, \mathbf{B}_{-t}) \propto \delta(V_{t}, U_{t}) + \frac{\delta(V_{t}, u^{*})\omega_{-t}\mu_{t-1}(V_{t})}{\chi_{-t} + \omega_{-t}} \sum_{u \in \widetilde{\mathcal{N}}(V_{t})} \left[Q_{t-1}^{\kappa_{-t}, \bar{\tau}_{-t}} \right]_{V_{t}, u}$$

with $Q_{t-1}^{\kappa_{-t},\bar{\tau}_{-t}}$ as in (20) with $r = \kappa_{-t}$, $p = \bar{\tau}_{-t}$. The updates for **K** are

$$P(K_{t} = k \mid G_{(t-1):t}, \mathbf{K}_{-t}, \mathbf{B}_{-t}) \propto \frac{\Gamma(\kappa_{-t} + k)}{\Gamma(k+1)\Gamma(\kappa_{-t})} (1 - \bar{\tau}_{-t})^{\kappa_{-t}} \bar{\tau}_{-t}^{k} \dots$$

$$\times \left[\delta_{t}(V_{t}, u^{*}) \mu_{t-1}(V_{t}) \left(\frac{\chi_{-t}}{\chi_{-t} + \omega_{-t}} + \frac{\omega_{-t}}{\chi_{-t} + \omega_{-t}} \sum_{u \in \widetilde{\mathcal{N}}(V_{t})} \left[Q_{t-1}^{k+1} \right]_{V_{t}, u} \right) \dots \right]$$

$$+ \delta_{t}(V_{t}, U_{t}) \frac{\omega_{-t}}{\chi_{-t} + \omega_{-t}} \left(\mu_{t-1}(V_{t}) \left[Q_{t-1}^{k+1} \right]_{V_{t}, U_{t}} + \mu_{t-1}(U_{t}) \left[Q_{t-1}^{k+1} \right]_{U_{t}, V_{t}} \right) \right]$$

with $Q_{t-1}^{k+1} = D_{t-1}^{-1/2}(\mathbb{I}_{t-1} - \mathbf{L}_{t-1})^{k+1}D_{t-1}^{1/2}$, the probability of a random walk of length k+1 from u to v. For implementation, the distribution for K_t must be truncated at some finite k, which can safely be done at three or four times the diameter of G_T : The total remaining probability mass can be calculated analytically, and the mass is placed on larger k is negligible.

Sampling $G_{2:(T-1)}$. Implementation of Algorithm 2 is straight-forward, with one exception: at each SMC step $G_{t-1} \to G_t$, we collapse the dependence on the particular values of B_t, K_t in that sampling iteration so that edges are proposed from the collapsed transition kernel $q_{\alpha,\lambda}^t(G_t | G_{t-1}, \mathbf{B}_{-t}, \mathbf{K}_{-t})$. Thus, G_t is composed of G_{t-1} plus a random edge e_t sampled as

$$P(e_{t} = (v, u)) \propto \\ \mathbb{1}\{(v, u) = (V_{t}, u^{*})\}\mu_{t-1}(v) \left(\frac{\chi_{-t}}{\chi_{-t} + \omega_{-t}} + \frac{\omega_{-t}}{\chi_{-t} + \omega_{-t}} \left(\sum_{u \in \widetilde{\mathcal{N}}(v)} \left[Q_{t-1}^{\kappa_{-t}, \overline{\tau}_{-t}}\right]_{v, u}\right)\right) + \dots$$

$$\mathbb{1}\{(v, u) = (V_{t}, U_{t})\}\frac{\omega_{-t}}{\chi_{-t} + \omega_{-t}} \left(\mu_{t-1}(v) \left[Q_{t-1}^{\kappa_{-t}, \overline{\tau}_{-t}}\right]_{v, u} + \mu_{t-1}(u) \left[Q_{t-1}^{\kappa_{-t}, \overline{\tau}_{-t}}\right]_{u, v}\right).$$

APPENDIX C: SENSITIVITY TO PRIOR SPECIFICATION

Since the MCMC approach requires prior distributions on the model parameters α and λ , we have to consider how different choices of priors imply assumptions on the graph structure, and how they affect inference. Interpreting α is straightforward, as an expected ratio of vertices to edges (see also Figure 1). Since it also has compact domain, the experiments reported in this section draw it from a uniform prior. Of interest here is the influence of λ . The following tables report the empirical mean of several pertinent statistics, computed on graphs generated from the model using a gamma prior with parameters $(a_{\lambda},b_{\lambda})$. Standard deviations are computed over 100 realizations of a simple graph with 500 edges.

$\mathbf{RW}_{^{\mathrm{U}}}\;(a_{\lambda},b_{\lambda})$	$\mathbb{E}[\lambda]$	$\mathrm{Var}[\lambda]$	Diameter	$Avg.\ SP$	Clustering coeff.	Vertices	$\max(\deg)$	$\overline{\deg}$
(1.000, 0.250)	4	16	16.53 (4.7)	6.98 (2.1)	0.1379 (0.088)	375.2 (107)	17.1 (7.4)	3.02 (1.3)
(4.000, 1.000)	4	4	16.31 (4.4)	6.81(2.0)	0.1486 (0.084)	365.6 (99)	17.6 (7.0)	3.01(1.1)
(1.000, 1.000)	1	1	19.01 (3.3)	7.98 (1.4)	0.1665 (0.097)	417.9 (67)	14.5(4.2)	2.47(0.5)
(0.001, 0.001)	1	1000	21.87 (1.7)	9.62(0.5)	0.0000 (0.000)	501.0(0)	9.6(1.3)	2.00(0.0)
$\mathbf{RW}_{\text{\tiny SB}}\ (a_{\lambda},b_{\lambda})$	$\mathbb{E}[\lambda]$	$\mathrm{Var}[\lambda]$	Diameter	Avg. SP	Clustering coeff.	Vertices	$\max(\deg)$	$\overline{\deg}$
$\frac{\mathbf{RW}_{SB} (a_{\lambda}, b_{\lambda})}{(1.000, 0.250)}$	$\frac{\mathbb{E}[\lambda]}{4}$	$Var[\lambda]$ 16	Diameter 11.28 (3.0)	Avg. SP 4.71 (1.1)	Clustering coeff. 0.1938 (0.117)	Vertices 395.9 (84)	max(deg) 58.1 (18.4)	$\frac{\overline{\text{deg}}}{2.67 \ (0.7)}$
	. ,				5 50		(0,	
(1.000, 0.250)	4	16	11.28 (3.0)	4.71 (1.1)	0.1938 (0.117)	395.9 (84)	58.1 (18.4)	2.67 (0.7)

The differences between the RW_U and RW_{SB} model are clearly visible: Regardless of prior choice, the latter tends to have smaller diameter and average shortest path length, and a higher clustering coefficient. Figure 9 shows averages for three of these statistics generated with fixed parameter values.

The last row of either table, with parameters (0.001, 0.001), corresponds to a gamma distribution commonly used as a "non-informative" prior in Bayesian analysis, and exhibits a phenomenon often observed for such priors: On the one hand, the prior places most of its mass near 0, with the result that simulation from the prior tends to produce very small parameters values. In our model, such small values of λ generate a tree-like graph (note the number of vertices in all experiments is exactly 501, for 500 edges). On the other hand, the tail of the prior decays sufficiently slowly that even a small sample can pull the posterior away from 0, and indeed parameter updates in the Gibbs sampler are nearly equal to the MLE of λ based on the latent walk lengths \mathbf{K} .

More generally, the definition of the model implies that the posterior should peak somewhere between zero to the mixing time of the random walk. More important for inference than the prior's shape is hence that it does not exclude this region from its support, and as a rule of thumb, any prior that spreads its mass well over the interval between 0 and 2-3 times the diameter of the network can be expected to yield reasonable results in most cases.

In order to study the sensitivity of posterior inference to prior specification, we vary the prior distribution parameters and use the particle Gibbs sampler to fit the $\mathbf{RW}_{\text{SB}}(\alpha,\lambda)$ model to synthetic graphs of two difference sizes (T=50 and T=100). Figure 10 show 1000 samples collected after 500 burn-in iterations, each run for combinations of three different priors on α and λ . As one would expect,

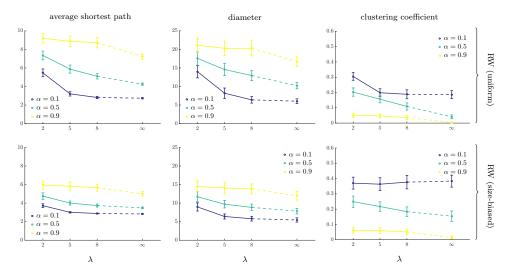


FIG 9. Statistics (average shortest path, diameter, clustering coefficient) of simple graphs with 500 edges generated by the random walk model. Averages are over 100 samples and error bars are plus/minus one standard error. $\lambda = \infty$ corresponds to the limiting ACL model (see Section 3.4).

problems arise if the prior peaks sharply at a value far away from the true parameter value. In the absence of strong prior knowledge, it is hence advisable to choose reasonably uninformative priors. In particular, the beta prior on α should usually be chosen as uniform. If the prior on α has a distinctive peak, it may distort posterior inference, particularly in small data settings. For example, the bottom row of Figure 10 (bottom) shows this effect.

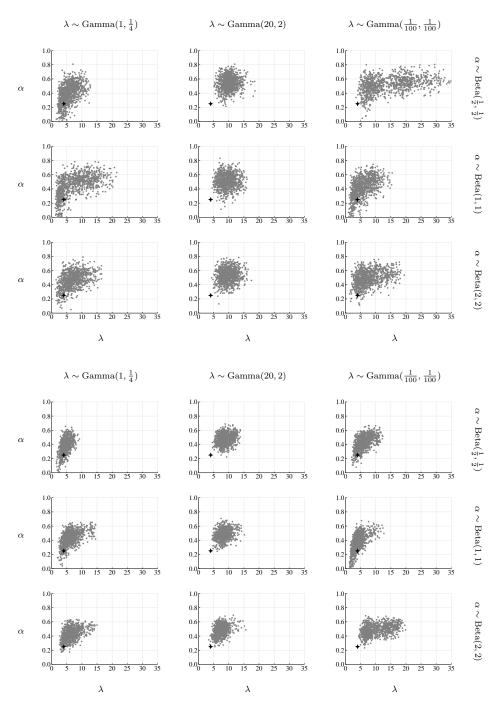


Fig 10. Prior sensitivity, for sample graphs of size T=50 (top) and T=100 (bottom). Grey dots are posterior samples; the black star indicates the parameter values used to generate the data.

REFERENCES

- [1] Aiello, W., Chung, F., and Lu, L. (2002). Random evolution in massive graphs. In *Handbook of Massive Data Sets*, volume II, pages 97–122.
- [2] Ambroise, C. and Matias, C. (2012). New consistent and asymptotically normal parameter estimates for random-graph mixture models. J. R. Stat. Soc. Ser. B, 74(1), 3–35.
- [3] Andrieu, C., Doucet, A., and Holenstein, R. (2010). Particle markov chain Monte Carlo methods. J. R. Stat. Soc. Ser. B, 72(3), 269–342.
- [4] Barabási, A.-L. and Albert, R. (1999). Emergence of scaling in random networks. Science, 186(5439), 509-512.
- [5] Batagelj, V. and Mrvar, A. (2006). Pajek datasets. http://vlado.fmf.uni-lj.si.
- [6] Bickel, P. J., Chen, A., and Levina, E. (2011). The method of moments and degree distributions for network models. *Ann. Statist.*, **39**(5), 2280–2301.
- [7] Bloem-Reddy, B. and Orbanz, P. (2017). Preferential attachment and vertex arrival times. arXiv 1710.02159.
- [8] Bloem-Reddy, B., Foster, A., Mathieu, E., and Teh, Y. W. (2018). Sampling and inference for Beta Neutral-to-the-Left models of sparse networks. In *Uncertainty in Artificial Intelligence*.
- [9] Borgs, C., Chayes, J. T., Lovász, L., Sós, V. T., and Vesztergombi, K. (2008). Convergent sequences of dense graphs. I. Adv. Math., 219(6), 1801–1851.
- [10] Borgs, C., Chayes, J. T., Cohn, H., and Zhao, Y. (2014). An L^p theory of sparse graph convergence I: limits, sparse random graph models and power law distributions.
- [11] Box, G. E. P. (1980). Sampling and Bayes' inference in scientific modelling and robustness. J. R. Stat. Soc. Ser. A, 143(4), pp. 383–430.
- [12] Bubeck, S., Mossel, E., and Racz, M. Z. (2015). On the influence of the seed graph in the preferential attachment model. *IEEE Trans. Network Sci. Eng.*, **2**(1), 30–39.
- [13] Butland, G., Peregrin-Alvarez, J. M., Li, J., Yang, W., Yang, X., Canadien, V., Starostine, A., Richards, D., Beattie, B., Krogan, N., Davey, M., Parkinson, J., Greenblatt, J., and Emili, A. (2005). Interaction network containing conserved and essential protein complexes in escherichia coli. *Nature*, 433(7025), 531–537.
- [14] Cai, D., Campbell, T., and Broderick, T. (2016). Edge-exchangeable graphs and sparsity. In Adv. Neural Inf. Process. Syst. 29, pages 4242–4250.
- [15] Caron, F. and Fox, E. B. (2017). Sparse graphs using exchangeable random measures. J. R. Stat. Soc. Ser. B, 79(5), 1–44.
- [16] Chung, F. (1997). Spectral Graph Theory (CBMS Regional Conference Series in Mathematics, No. 92). American Mathematical Society.
- [17] Chung, F. and Lu, L. (2006). Complex Graphs and Networks. (CBMS Regional Conference Series in Mathematics). American Mathematical Society.
- [18] Chung, F. and Yau, S.-T. (2000). Discrete Green's functions. J. Combin. Theory Ser. A, $\bf 91(1-2)$, 191-214.
- [19] Crane, H. and Dempsey, W. (2017). Edge exchangeable models for interaction networks. J. Amer. Statist. Assoc. In press.
- [20] Del Moral, P. and Murray, L. M. (2015). Sequential Monte Carlo with highly informative observations. SIAM J. Uncertainty Quantification, 3(1), 969–997.
- [21] Doucet, A. and Johansen, A. M. (2011). A tutorial on particle filtering and smoothing: fifteen years later. Oxford Handbook of Nonlinear Filtering, pages 656–704.
- [22] Durrett, R. (2006). Random Graph Dynamics. Cambridge University Press.
- [23] Fearnhead, P. and Clifford, P. (2003). Online inference for hidden Markov models via particle filters. Journal of the Royal Statistical Society: Series B (Statistical Methodology), 65(4), 887– 899.
- [24] Gao, C., Lu, Y., and Zhou, H. H. (2015). Rate-optimal graphon estimation. Ann. Statist., 43, 2624–2652.
- [25] Gelman, A., Meng, X., and Stern, H. (1996). Posterior predictive assessment of model fitness via realized discrepancies. Statist. Sinica, 6(4), 733–807.
- [26] Globerson, A., Chechik, G., Pereira, F., and Tishby, N. (2007). Euclidean Embedding of Co-occurrence Data. J. Mach. Learn. Res., 8, 2265–2295.
- [27] Goldenberg, A., Zheng, A., Fienberg, S., and Airoldi, E. (2010). A survey of statistical network models. Found. Trends Machine Learning, 2(2), 129–233.
- [28] Griffiths, R. and Tavaré, S. (1994). Simulating probability distributions in the coalescent.

- Theoretical Population Biology, 46(2), 131 159.
- [29] Hoff, P. (2008). Modeling homophily and stochastic equivalence in symmetric relational data. In Adv. Neural Inf. Process. Syst. 20, pages 657–664.
- [30] Hoff, P. D., Raftery, A. E., and Handcock, M. S. (2002). Latent space approaches to social network analysis. J. Amer. Statist. Assoc, 97(460), 1090–1098.
- [31] Hunter, D. R., Goodreau, S. M., and Handcock, M. S. (2008). Goodness of fit of social network models. J. Amer. Statist. Assoc, 103(481), 248–258.
- [32] James, L. F. (2015). Generalized Mittag-Leffler distributions arising as limits in preferential attachment models. arXiv 1509.07150.
- [33] Janson, S. (2017). On edge exchangeable random graphs. arXiv 1702.06396.
- [34] Jasra, A., Persing, A., Beskos, A., Heine, K., and De Iorio, M. (2015). Bayesian inference for duplication—mutation with complementarity network models. *Journal of Computational Biology*, 22(11), 1025–1033.
- [35] Kemp, C., Tenenbaum, J., Griffiths, T., Yamada, T., and Ueda, N. (2006). Learning systems of concepts with an infinite relational model. In Proc. AAAI'06, pages 381–388.
- [36] Kolaczyk, E. D. (2009). Statistical Analysis of Network Data. Springer-Verlag.
- [37] Koskinen, J. H. and Snijders, T. A. (2007). Bayesian inference for dynamic social network data. Journal of Statistical Planning and Inference, 137(12), 3930–3938.
- [38] Lafferty, J. and Lebanon, G. (2005). Diffusion kernels on statistical manifolds. J. Mach. Learn. Res., 6, 129–163.
- [39] Liggett, T. M. (2005). Interacting particle systems. Springer.
- [40] Loomis, C. P., Morales, J. O., Clifford, R. A., and Leonard, O. E. (1953). Turrialba: Social Systems and the Introduction of Change. The Free Press, Glencoe, Ill.
- [41] Minhas, S., Hoff, P. D., and Ward, M. D. (2016). A new approach to analyzing coevolving longitudinal networks in international relations. *J. Peace Research*, **53**(3), 491–505.
- [42] Móri, T. F. (2005). The maximum degree of the Barabási–Albért random tree. Comb. Probab. Comput., 14(3), 339–348.
- [43] Navlakha, S. and Kingsford, C. (2011). Network archaeology: uncovering ancient networks from present-day interactions. PLoS computational biology, 7(4), e1001119.
- [44] Newman, M. (2009). Networks. An Introduction. Oxford University Press.
- [45] Orbanz, P. and Roy, D. M. (2015). Bayesian models of graphs, arrays and other exchangeable random structures. *IEEE PAMI*, 37, 437–461.
- [46] Peköz, E. A., Röllin, A., and Ross, N. (2017). Joint degree distributions of preferential attachment random graphs. *Adv. in Appl. Probab.*, **49**(2), 368–387.
- [47] Pitman, J. (2006). Combinatorial Stochastic Processes. Springer.
- [48] Pitt, M., Silva, R., Giordani, P., and Kohn, R. (2010). Auxiliary particle filtering within adaptive Metropolis-Hastings sampling. arXiv 1006.1914.
- [49] Pons, P. and Latapy, M. (2006). Computing communities in large networks using random walks. J. Graph Algorithms Appl., 10(2), 191–218.
- [50] Robert, C. P. and Casella, G. (2004). Monte Carlo Statistical Methods. Springer.
- [51] Smola, A. J. and Kondor, I. (2003). Kernels and regularization on graphs. In Proc. Annual Conference on Computational Learning Theory. Springer.
- [52] Thorne, T. and Stumpf, M. P. H. (2012). Graph spectral analysis of protein interaction network evolution. J. R. Soc. Interface.
- [53] Tomasello, M. V., Perra, N., Tessone, C. J., Karsai, M., and Schweitzer, F. (2014). The role of endogenous and exogenous mechanisms in the formation of R&D networks. *Scientific Reports*, 4. Article 5679.
- [54] Vishwanathan, S. V. N., Schraudolph, N. N., Kondor, R., and Borgwardt, K. M. (2010). Graph kernels. J. Mach. Learn. Res., 11, 1201–1242.
- [55] Wang, J., Jasra, A., and De Iorio, M. (2014). Computational methods for a class of network models. J. Comput. Biol., 21(2), 141–161.
- [56] Williamson, S. A. (2016). Nonparametric network models for link prediction. J. Mach. Learn. Res., 17(202), 1–21.
- [57] Wiuf, C., Brameier, M., Hagberg, O., and Stumpf, M. P. H. (2006). A likelihood approach to analysis of network data. Proc. Natl. Acad. Sci., 103(20), 7566–7570.
- [58] Wolfe, P. J. and Olhede, S. C. (2013). Nonparametric graphon estimation. arXiv 1309.5936.
- [59] Young, J.-G., Hébert-Dufresne, L., Laurence, E., Murphy, C., St-Onge, G., and Desrosiers,

P. (2018). Network archaeology: phase transition in the recoverability of network history. arXiv 1803.09191.

[60] Zhou, M. (2015). Infinite edge partition models for overlapping community detection and link prediction. In Proceedings of the Eighteenth International Conference on Artificial Intelligence and Statistics, volume 38, pages 1135–1143.

DEPARTMENT OF STATISTICS 24–29 St. Giles' Oxford OX1 3LB, UK

 $\hbox{E-MAIL: benjamin.bloem-reddy@stats.ox.ac.uk}\\$

DEPARTMENT OF STATISTICS 1255 AMSTERDAM AVENUE NEW YORK, NY 10027, USA

 $\hbox{E-MAIL: porbanz@stat.columbia.edu}\\$